THE INFLUENCE OF DRILLED CAVITIES ON NATURAL CONVECTION HEAT TRANSFER FROM A HORIZONTAL SURFACE

Le Vinh Hiep

NAVAL POSTGRADUATE SCHOOL
Monterey, California

THESIS

The Influence of Drilled Cavities On
Natural Convection Heat Transfer
From a Horizontal Surface

by

Le Vinh Hiep

June 1975

Thesis Advisor: M. D. Kelleher

Approved for public release; distribution unlimited.

SECURITY CLASSIFICATION OF THIS PAGE (When Data Entered)

REPORT DOCUMENTATION PAGE		READ INSTRUCTIONS BEFORE COMPLETING FORM
1. REPORT NUMBER	2. GOVT ACCESSION NO.	3. RECIPIENT'S CATALOG NUMBER
4. TITLE (and Subtitle) The Influence of Drilled Cavities on Natural Convection Heat Transfer From a Horizontal Surface		5. TYPE OF REPORT & PERIOD COVERED Master's Thesis June 1975 6. PERFORMING ORG. REPORT NUMBER
7. AUTHOR(s) Le Vinh Hiep		8. CONTRACT OR GRANT NUMBER(s)
9. PERFORMING ORGANIZATION NAME AND ADDRESS Naval Postgraduate School Monterey, California 93940		10. PROGRAM ELEMENT, PROJECT, TASK AREA & WORK UNIT NUMBERS
11. CONTROLLING OFFICE NAME AND ADDRESS Naval Postgraduate School Monterey, California 93940		12. REPORT DATE June 1975 13. NUMBER OF PAGES
14. MONITORING AGENCY NAME & ADDRESS(if different from Controlling Office)		15. SECURITY CLASS. (of this report) Unclassified 15a. DECLASSIFICATION/DOWNGRADING SCHEDULE

16. DISTRIBUTION STATEMENT (of this Report)

Approved for public release; distribution unlimited.

17. DISTRIBUTION STATEMENT (of the abstract entered in Block 20, if different from Report)

18. SUPPLEMENTARY NOTES

19. KEY WORDS (Continue on reverse side if necessary and identify by block number)

20. ABSTRACT (Continue on reverse side if necessary and identify by block number)

The objective of this project was to study the effect that small artificial cavities have on natural convection from a horizontal surface. Tests were run with water and Freon 113. Data for heat flux as a function of bulk temperature difference were carefully obtained. These data yielded Nusselt number as a function of Grashof number or Rayleigh number. All of these were then compared with the data obtained by O'Connor

[Ref. 3]. Experimental results are presented for the heat transfer from horizontal circular disks, with and without artificial cavities.

The data from a mirror finished surface was compared to that of previous investigations and the agreement was good. The artificial cavities were found to affect the natural convection heat transfer from a horizontal surface: the heat transfer coefficients in both cases (water and Freon 113) were decreased.

THE INFLUENCE OF DRILLED CAVITIES ON NATURAL CONVECTION HEAT TRANSFER FROM A HORIZONTAL SURFACE

by

Le Vinh Hiep
B.S., Naval Postgraduate School, 1975

Submitted in partial fulfillment of the
requirements for the degree of

MASTER OF SCIENCE IN MECHANICAL ENGINEERING

from the

NAVAL POSTGRADUATE SCHOOL
June 1975

ABSTRACT

The objective of this project was to study the effect that small artificial cavities have on natural convection from a horizontal surface. Tests were run with water and Freon 113. Data for heat flux as a function of bulk temperature difference were carefully obtained. These data yielded Nusselt number as a function of Grashof number or Rayleigh number. All of these were then compared with the data obtained by O'Connor [Ref. 3]. Experimental results are presented for the heat transfer from horizontal circular disks, with and without artificial cavities.

The data from a mirror finished surface was compared to that of previous investigations and the agreement was good. The artificial cavities were found to affect the natural convection heat transfer from a horizontal surface: the heat transfer coefficients in both cases (water and Freon 113) were decreased.

TABLE OF CONTENTS

LIST OF TABLES

LIST OF FIGURES

NOMENCLATURE

SYMBOL	DESCRIPTION	UNITS
D	Heater Surface Diameter	Inches or ft
g	Acceleration of Gravity	$Ft/_{sec^2}$
h	Convection Heat Transfer Coefficient	$BTU/Hr/Ft^2/^oF$
H	Height of Cylindrical Tank	Inches or ft
K_{ss}	Thermal Conductivity of 304 Stainless Steel	$BTU/Hr/Ft/^oF$
K_f	Thermal Conductivity of Test-Fluid Distilled Water or Freon 113	$BTU/Hr/Ft/^oF$
R	Radius of Cylindrical Tank	Inches or ft
T_b	Bulk Temperature of Fluid	^oF
T_s	Test Section Surface Temperature	^oF
δT	Temperature Difference Between Test Surface and Fluid ($T_s - T_b$)	^oF
T_o	Temperature Measured in Stainless Steel Test Section at a Location 0.227 inch from Test Surface	^oF
T_1	Temperature Measured in Stainless Steel Test Section 0.750 inch from Test Surface	^oF
δT_{ss}	Temperature Difference in Test Section ($T_1 - T_o$)	
T_f	Film Temperature $\frac{T_s + T_b}{2}$	^oF
δx	Distance in Stainless Steel Section Between Thermocouple No. 1 and Thermocouple No. 0	Inches or ft

$U_{Subscript}$	Uncertainty in Variables Denoted by Subscript, for Example: $W_{T_{ss}}$ in T_{ss}	Units of variables denoted by subscript
α	Fluid Thermal Diffusivity	Ft^2/sec
β	Fluid Coefficient of Thermal Expansion	$1/^oF$
ν	Fluid Kinematic Viscosity	Ft^2/sec

DIMENSIONLESS NUMBERS

Nu	Nusselt Number Based on Test Section Diameter	hD/K_f
Pr	Fluid Praudtl Number	ν/α
Gr	Grashof Number Based on Test Surface Diameter	$\frac{g\beta D^3 \delta T}{\nu^2}$
Gr_H	Grashof Number Based on Cylindrical Tank Radius	$\frac{g\beta R^3 \delta T}{\nu^2}$
Ra	Rayleigh Number	$Gr \cdot Pr$
P	Power into Heater	Watt

ACKNOWLEDGMENT

The author wishes to express his appreciation to Dr. M. D. Kelleher, Professor of Mechanical Engineering, Naval Postgraduate School, for his assistance, encouragement and the unselfish giving of his time. Without his perserverance this work could not have been completed.

He would like to thank Mr. Tom Christian, Mr. George Bixler, Mr. Jack McKay, Mr. Roy Edwards and all of the Mechanical Engineering Department for their advice and work on design of the experimental apparatus.

The author also expresses his gratitude to Professor Paul Marto, Professor Thomas Copper, Professor Dong Nguyen for their advice and assistance.

A special word of thanks and sincere appreciation to his fiancee, Kim-Thoa, for a long time and encouragement waiting. Thank God for her presence with him.

I. INTRODUCTION

A. BACKGROUND

Some recent experimental data with liquid nitrogen showed that drilled cavities in a horizontal disk can improve the heat transfer coefficient during free convection [Ref. 1]. These cavities were approximately 0.015 inches in diameter and 0.025 inches deep, and were placed in a copper mirror finished, surface. Tests were run with none, one, seven and thirteen cavities and the heat transfer coefficient continued to improve as the number of cavities were increased.

Free convection heat transfer occurs when a body is placed in a fluid at a higher or lower temperature than that of the body. The difference in temperature implies that heat flows between the fluid and the body and also causes a change in the density of the fluid layers in the vicinity of the surface. On account of thermal expansion, the fluid at the bottom will be lighter than the fluid at the top. Because of this there will be a tendency on the part of the fluid to redistribute itself, however, this natural tendency on the part of the fluid will be inhibited by its own viscosity. The difference in density leads to downward flow of the heavier fluid and upward flow of the lighter. In both free and forced convection, the currents transfer internal energy stored in the fluid, however, the intensity of the mixing motion is generally greater in forced convection so the heat

transfer coefficients are greater than in free convection. The heat transfer coefficients in free convection are relatively low but good enough for cooling many devices in the electrical engineering field: transformers, rectifiers, transmission line, electrically heated wires as in incandescent lamps and the heating elements of an electric furnace. Free convection heat transfer plays an important role in steam radiators, wall of a building, especially on the stationary human body in a quiescent atmosphere. A knowledge of free convection heat transfer coefficients is necessary to understand and determine the heat load on air-conditioning or refregeration equipments. Free convection causes the heat losses from pipes or other heated fluids, to cool the surfaces of bodies in which heat is generated by fission [Ref. 2] in nuclear power applications.

This experiment examines the effects of surface cavities on heat transfer from a horizontal surface with water and Freon 113.

A geometrical configuration should be a first step in studying the natural convection in enclosures. The geometry and power input situations vary throughout the literature of studying the natural convection in enclosures. To start this experiment, a circular test section in a cylindrical container, with the same size for radius of the tank and height of the tank was used. Heat transfer data could be compared with existing results, especially with O'Connor's [Ref. 3].

The heat transfer across plane vertical and horizontal layers of gas, as well as across annular spaces, is most interesting from the point of view of applications. In this kind of study, we find the problem of insulation by air layers, as well as the heat transfer through porous materials. The boundary layer thickness are no longer small in comparison with the dimensions of the air space so that the development of the flow is often strongly influenced by the shape of the boundaries. An unstable stratification is formed if the heat flow is directed upward and the lower density fluid is located below the cooler fluid (density is higher). This unstable stratification must breakdown at a certain value of Rayleigh number (Gr·Pr) above which a convective motion must be generated [Ref. 4], Jeffreys [Ref. 5] and Low [Ref. 6] calculated this limiting value of Rayleigh number and the value was 1700 in case of the air layer is bounded on both sides by solid walls and a value of 1108 was found with a free upper surface. Schmidt and Saunders [Ref. 7] carried out an optical investigation in a trough filled with water and have confirmed the first of these values very satisfactorily. When the Rayleigh number is above the critical value, the convective motion in the fluid takes the form of quite regular hexagonals cells (also called Bénard cells), the fluid moves upward in the center and returns near the sides. In case of a horizontal layer with circular side walls, a concentric circular pattern of flow was obtained by Soberman [Ref. 8]. One method to describe the convective

heat transfer across a fluid layer is by an effective thermal conductivity Ke, which for a plane layer is defined by the equation [Ref. 9].

$$q = \frac{Ke}{\delta} (T_1 - T_2)$$

with Ke = thermal conductivity of a solid body which would admit the same heat flux as that occurring as a result of convection through the fluid layer of thickness δ under the action of a temperature difference $(T_1 - T_2)$ (T_1 and T_2 are the temperatures of the boundaries of the layer). Let K = the true thermal conductivity of the fluid then the ratio Ke/K describes the ralative increase in the heat transfer because of convection. Ke/K also represent the Nusselt number defined with respect to the length δ. The heat transfer across horizontal layers of air was measured by Mull and Reiher [Ref. 10] and the same measurements performed by Schmidt and Saunders [Ref. 7] with water (Pr = 7.1) at a Ra = 45000. The transition was quite sharp and could be easily determined. The curves for air and water do not coincide in a plot of Ke/K versus the Rayleigh number thus the true creeping motion can not be assumed, consequently Ra does not represent an appropriate dimensionless parameter. If a correlation of $Nu = C (Gr \cdot Pr^m)^n$ is applied to this case one obtains an approximate correlation of the data for air and water when m is put equal to 1.65. In the turbulent regime, the following equation is obtained

$$Nu = {}^{Ke}/_{K} = 0.073 (Gr \cdot Pr^{1.65})^{1/3}$$

valid for $Gr \cdot Pr^{1.65} > 160{,}000$. In the laminar region the scatter of the data is too great to permit a common correlation. In the case of air the onset of turbulence appears less well defined.

Torrance, et al [Ref. 11] designed an experimental model to study laminar flows induced by a simulated fire. They used air in a cylindrical enclosure with a heated disc in the center. Torrance, et al [Ref. 12], compared the experimental results with values determined from a numerical study. The Nusselt number based on a disc diameter versus the Grashof number was plotted. Excellent agreement between experimental and theoritical results were obtained. In this experimental work, turbulence occurred when the Grashof number (based on enclosure height), greater than 1.2×10^9. Lee and Hellman [Ref. 13] have a discussion on fire research in their papers.

The heat transfer from a horizontal circular disc, with a mirror finish in a cylindrical enclosure, was recorded by Duncan [Ref. 14] who obtained the following relation:

$$Nu = 0.31 \, (Ra)^{0.30}$$

and a comparison of his results with the results obtained by Torrance, et al [Ref. 12] theoritical and experimental was presented.

In 1968, P. J. Marto, J. A. Moulson, M. D. Maynard [Ref. 1] discussed the nucleate pool boiling of Nitrogen with different surface conditions. Pool boiling heat transfer of liquid nitrogen from circular, 1-in diameter horizontal disc was

studied. The surfaces were: copper and nickel mirror finishes, also copper surfaces roughened, grease-coated and Teflon-coated. Drilled cavities were cylindrical holes of diameter of 0.0043 and 0.015 inch and spark cut conical hole of 0.022 inch diameter. Surface roughness and material alter the nucleate-boiling curve and the Teflon-coated has very little effect while a grease coating significantly decreases the nucleate-boiling heat transfer coefficient. In this experiment, the effect of artificial cavities on both natural-convection and nucleate boiling was determined. Many data points were taken in the natural convection region.

In 1968, Torrance and Rockett [Ref. 12] made an analytical study of the natural convection induced in an enclosure by a small list spot centrally located on the floor. The enclosure was a circular cylinder, vertically oriented with a ratio of 1.0 for height over radius. A Prandtl number of 0.7 (air) was assumed and the Grashof number was based on the cylindrical height and list spot temperature. The equations of fluid flow in axisymmetric cylindrical coordinates were solved by numerical method with a computationally stable, explicit method. The computation were performed with starting conditions from quiescent through the initial transient to the fully developed flow. Solutions were obtained for Grashof number from 4×10^4 to 4×10^4. The flow patterns and temperature fields were illustrated with graphs displaying sets of streamlines and isotherms. With an extension of Grashof number to 4×10^{10}, a periodic vortex shielding developed, suggestive of the onset of instability.

The cited references and discussion have described what has been done in the area of natural convection in enclosures.

B. THESIS OBJECTIVES

The objectives of this work were:

1. To investigate the effects of drilled cavities on the natural convectin heat transfer in water and Freon 113.
2. To obtain natural convection heat transfer data from a mirror-like surface of circular geometry. The results would then be compared to that of Torrance, et al [Ref. 12] and also to the correlations of other investigators, especially with the results of O'Connor [Ref. 3].

This work would serve as a basis for future studies of natural convection heat transfer with different sizes and numbers of cavities and with different fluids.

II. EXPERIMENTAL APPARATUS

A. DESIGN CONSIDERATIONS

The test surface consisted of a stainless steel cylinder 0.895 inches in diameter installed in the center of a cylindrical tank 9.00 inches in diameter and 4.50 inches high so that it was flush with the tank floor. There are two test surfaces: one blank and one with seven drilled cavities. A controllable heat source (using resistance heaters) was housed in a copper block, and attached to this cylinder. A calibrated resistor in series with the heater was used to determine accurately the input power to the heater. Eight thermocouples, wired in series were used to measure the average bulk temperature of the fluid and one removable thermocouple was used to provide a check on this temperature. To record the temperature distribution of the stainless steel cylinder, four stainless steel sheathed thermocouples were equally spaced along the axis of the stainless steel test section. The temperatures at these locations were obtained using a Dana digital voltmeter. The test surface temperature was obtained by linearly extrapolating the two nearest thermocouples to the test surface (see Fig. 17).

Figure 1 is a cross sectional view of the tank, test section and heater assembly. Figure 2 is an overall view of the complete apparatus (including instrumentation).

Figure 3 shows a photograph of the two test section cylinders. The material for constructing of the tank, test section and heater arrangement were available from the apparatus used by O'Connor [Ref. 3].

The following criteria were used to establish the apparatus design:

(1) The enclosure radius was to be equal to the enclosure height. This ratio was convenient to work with and the results obtained could be directly compared to the experimental and theoritical results obtained by Torrance, et al [Ref. 12], Duncan [Ref. 14] and O'Connor [Ref. 3].

(2) The radius of the test surface was to be equal to one-tenth of the height of the enclosure, this is also the value used in the work of Torrance, et al [Ref. 11].

(3) The ratio of the depth cavity to diameter was approximately two, this corresponds to the value used by Moulson [Ref. 15].

Insulation was used to minimize the radial heat loss due to conduction as much as possible.

The test section designs used by Mac Kenzie [Ref. 16] and Duncan [Ref. 14] were examined. They both used a solid cylinder to get one dimentional heat flow. In Duncan's work, he used a stainless steel cylinder with a flanged top forming the test surface. Duncan [Ref. 14] discussed his results and showed the effects of heat transfer due to this design. Mac Kenzie [Ref. 16] used a similar cylinder-heater assembly in his work. To get one dimentional heat flow in cylinder we had to minimize the radial conduction losses. The cylinder would not be silver soldered to the heater section as O'Connor [Ref. 3] did, but a special design as

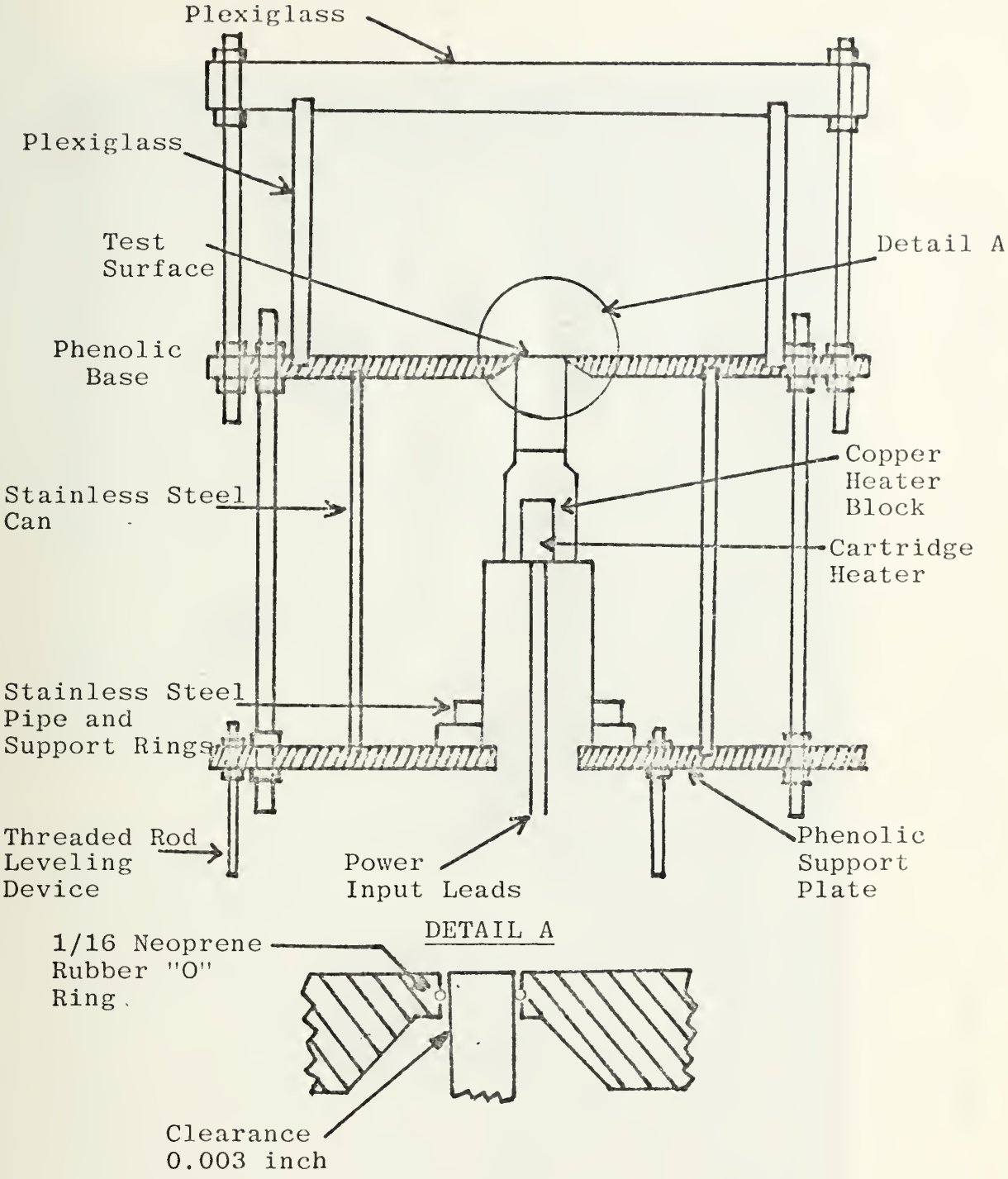

Figure 1. Cross Sectional View of Tank, Test Section and Heater Assembly.

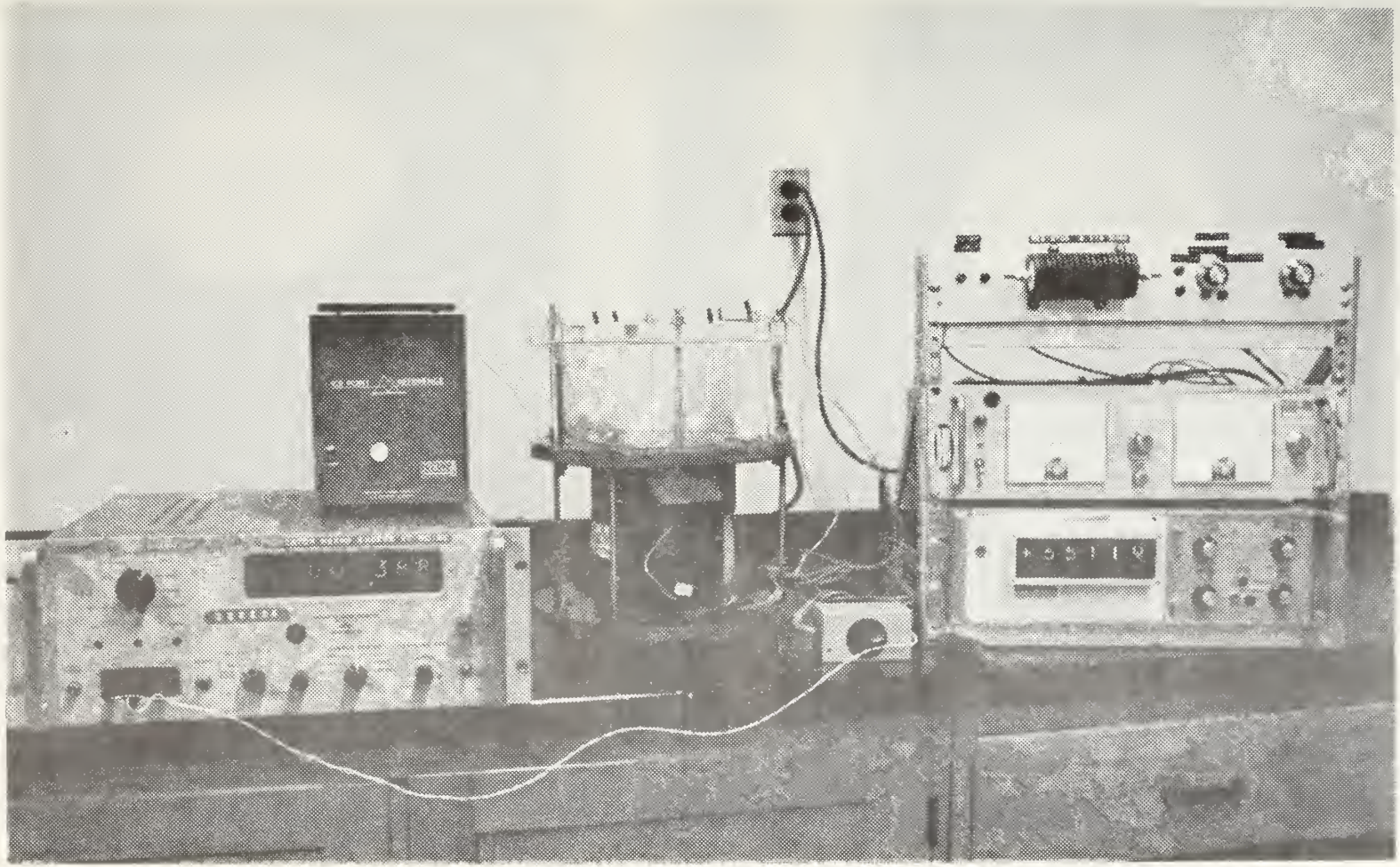

Figure 2. Photograph of Complete Apparatus Including Instrumentation.

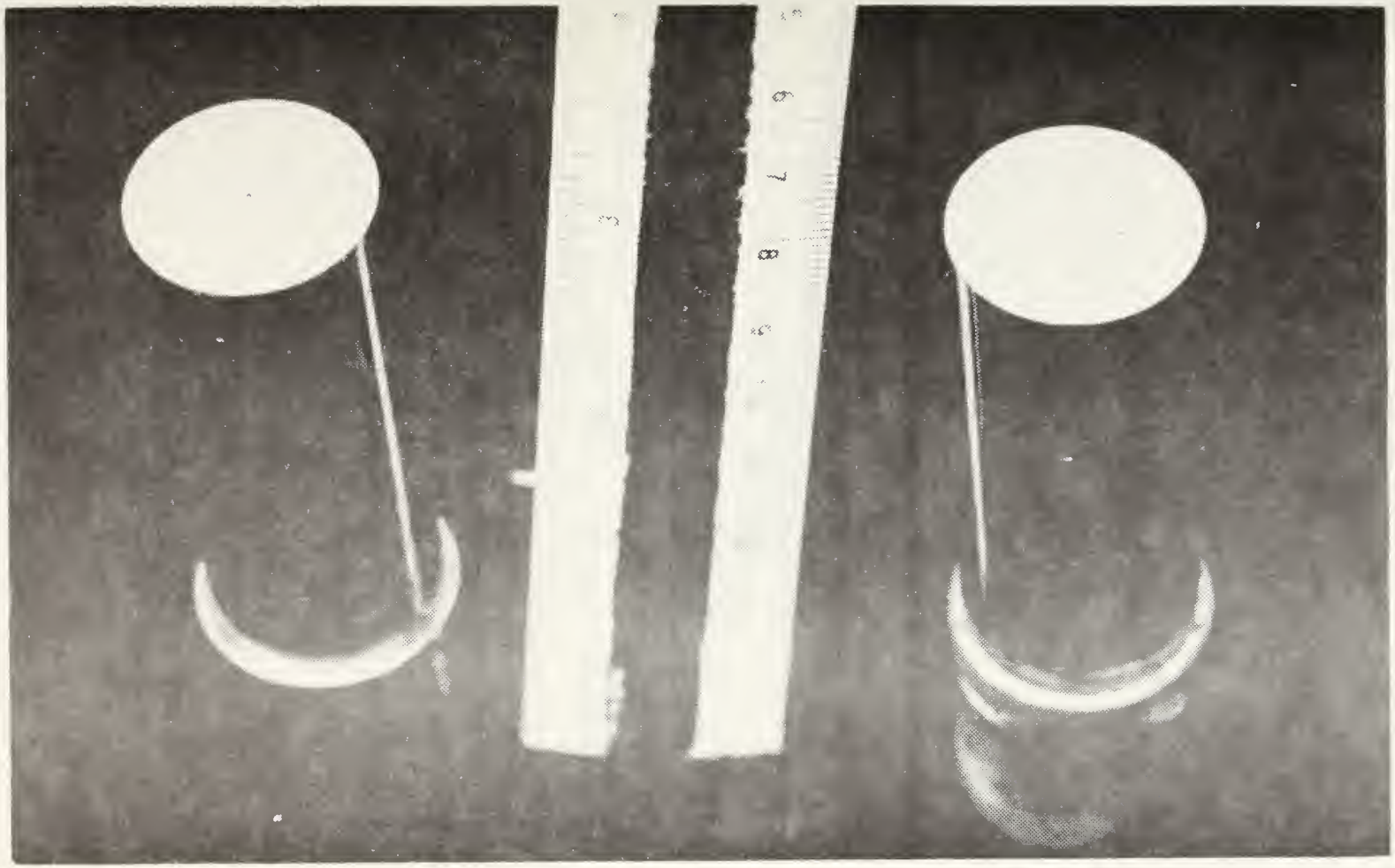

Figure 3. Photograph of the Two Test Sections.

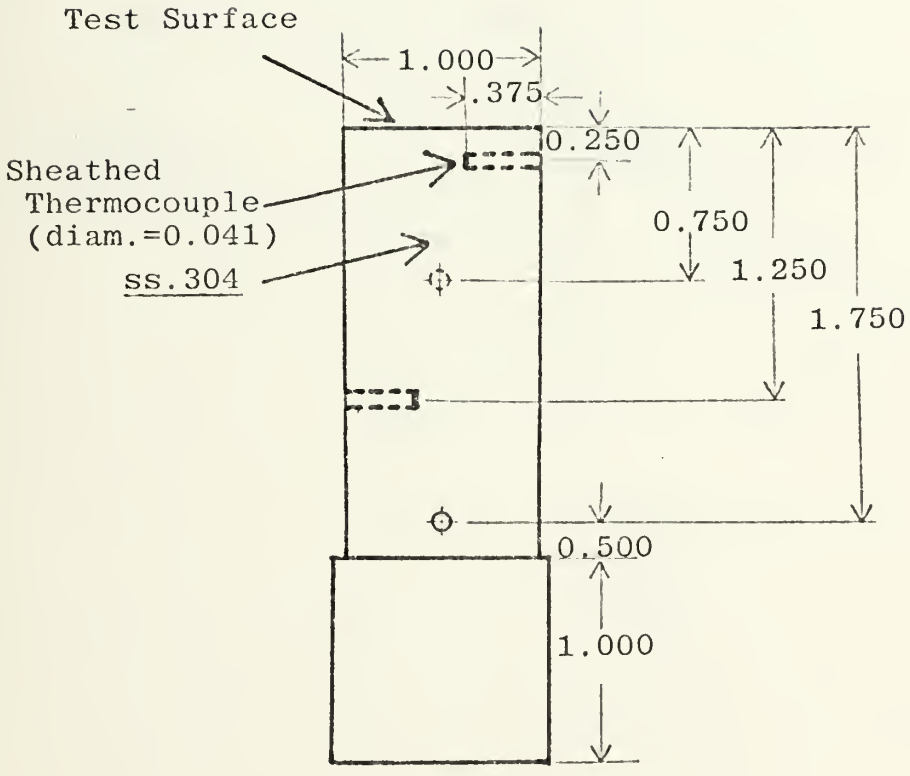

Figure 4. Blank Test Section.

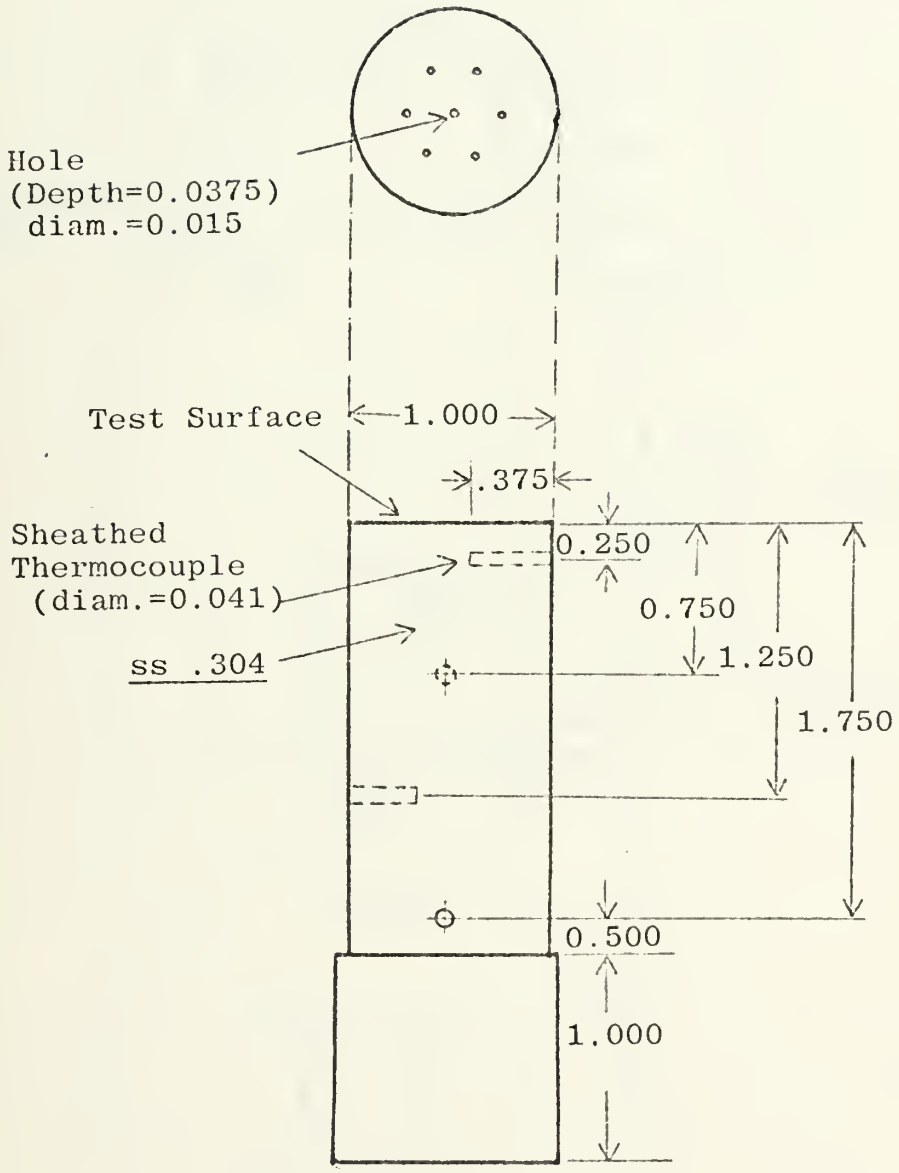

Figure 5. Seven-Hole Test Section.

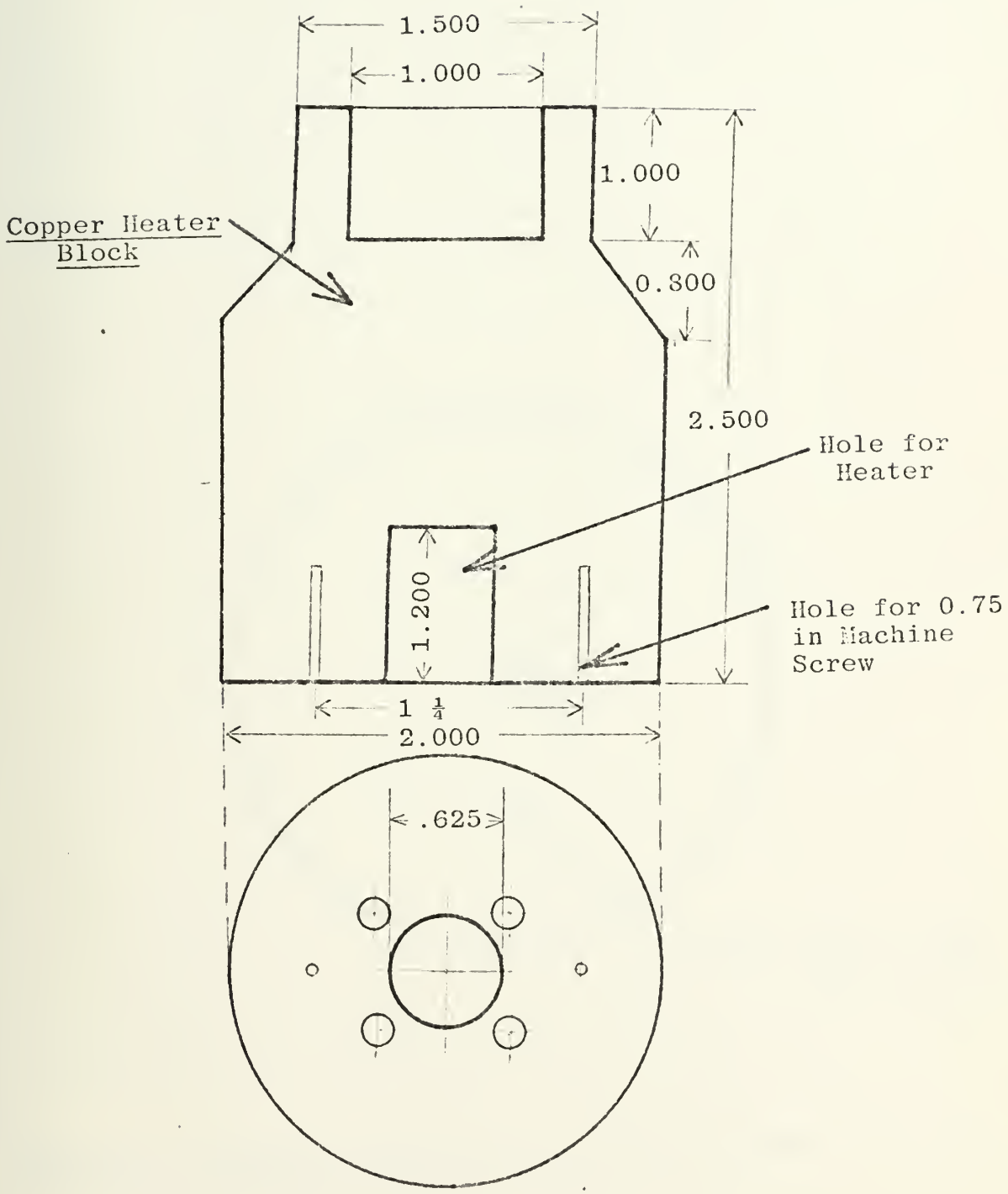

Figure 6. Test Section and Heater Assembly.

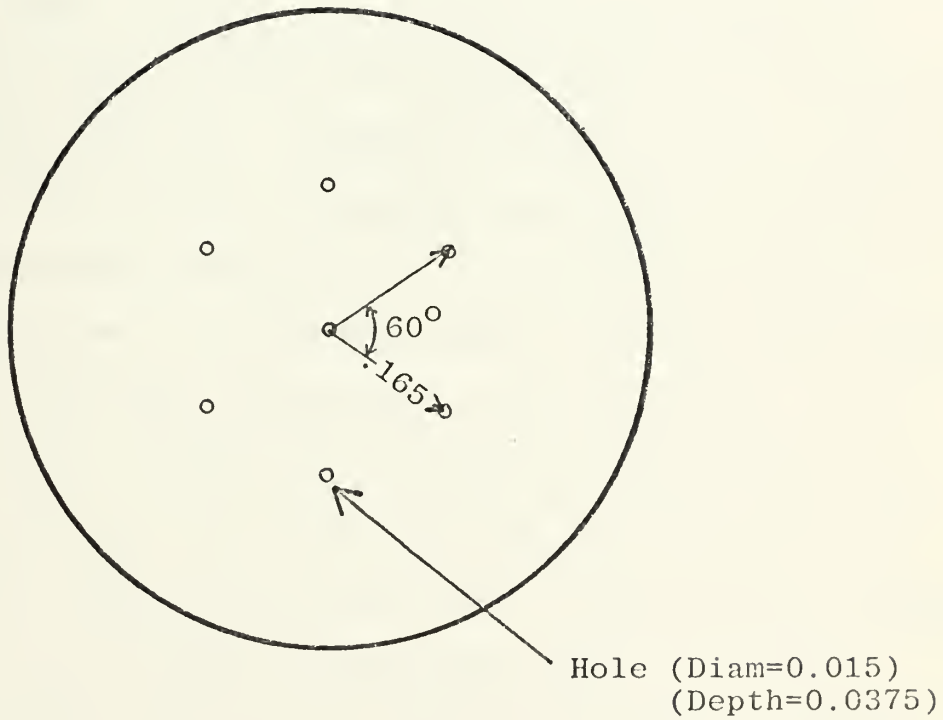

Figure 7. Layout of Seven-Hole Drilled Cavities.

shown in (Fig. 6) for a changeable cylinder test section was constructed. This test section-heater assembly would be rigidly supported at the base of the heater but also it could be raised or lowered by screws (see Fig. 6) to keep the test surface at the same level with the bottom surface of the tank. Because the heat flow through the cylinder would be the basis for the calculation of the convection heat-transfer coefficient (h), the thermal conductivity of the material used had to be accurately known. For this reason and because of its ease of machinability, 304 stainless steel was chosen for the test surface.

To minimize the heat loss by conduction through the bottom of the tank (since this bottom would be in contact with the test section), a material with a very low thermal conductivity was chosen. Phenolic was readily available and it was used by Mac Kenzie [Ref. 16] in a similar apparatus, thus it was known to be strong enough to resist the stresses applied in achieving a watertight tank arrangement. The stainless steel cylinder was centered in the bottom of the tank. To minimize the conduction area, the phenolic was machined to a tight fit and beveled. In the phenolic bottom plate (Fig. 1) a 0.0625 inch Neoprene rubber "O" ring, lubricated with silicone high vacuum grease was installed. Plexiglass was used for the tank top and sides.

B. TEST SECTION-HEATER ASSEMBLY

There were two test surfaces used in this experiment: one blank and one with seven cylindrical drilled cavities. The two-inch stainless steel cylinder (Fig. 3) was machined from a one-inch diameter 304 stainless steel rod to a .895 inch diameter. Four 0.041 inch diameter holes were drilled to a depth of 0.375 inch, separated axially approximately 0.5 inch and 90^0 apart for thermocouple installation. The stainless steel cylinder was attached to a copper block, by means of four screws to facilitate changing test sections (see Fig. 6). The copper block served as a housing for the heaters. To heat the test surface, five Watlow Firerod Cartridge were used, installed in the copper block. A 3.375 inch section of 2.0 inch diameter stainless steel tubing with a 2.0 inch outside and 0.625 inch inside diameter ring welded to one end was attached to the copper block and heater by two 0.75 inch machine screws, provided as a rigid support for the test section-heater assembly. This also eliminated the problem of metal to metal contact with the test section. In order to minimize the heat loss through this support, several holes were cut.

For seven-hole test section, seven cylindrical holes were drilled to a depth of 0.0375 inch and a diameter of 0.015 inch. Figure 7 is the layout of these seven holes on the test surface.

Several layers of asbestos paper were placed between the heater base and stainless steel ring. The stainless steel

rings machined to a tight fit to the pipe. These rings were bolted to a 12.0 inch diameter phenolic plate, which served as a support plate for the entire system. One end of the stainless steel pipe was fitted into the stainless steel ring. The test section-heater assembly was enclosed in a 0.125 inch thick steel can with a diameter of 6.25 inch.

It is important to minimize the heat loss from the test section and heater assembly.

Several layers of asbestos paper were wrapped around the heater assembly and a portion of the test section and secured with insulating tape. Several layers of Flex-Min K insulation were wrapped around the entire assembly, coupletely insulating the interior of the stainless steel can. Several layers of asbestos paper were put into the hole at the bottom of the stainless steel can, between the stainless steel ring holding the pipe section and the base plate (phenolic).

C. INSTRUMENTATION

1. Temperature Measurement

The accuracy of measurement of the temperatures was required for this experiment; so, ISA type T copper-constant, an thermocouples sheathed in stainless steel (sheath diameter diameter = 0.035 inch) were selected. The temperature distribution in the stainless steel section was determined using four of these thermocouples. The temperature of the surface was found using an extrapolating method (see Appendix II, Fig. 17).

The bulk temperature of the fluid was determined using eight Copper Coustantan thermocouples wired in series (four pairs) manufactured a Dynatech type of welder and a single removable thermocouple to provide a check on this temperature. The eight thermocouples were wired in series into an insulated switching box so the reading gave an average temperature. The sheathed thermocouple leads were securely fastened to the bottom phenolic plate of the assembly and the more plexible thermocouple extension wire was used to extend the wire into the switching box. A reference junction thermocouple was inserted in a sealed oil-filled glass tube which was immersed in a crushed ice-distilled water bath. This thermocouple was also wired into the switching box.

The output from the thermocouples was read on a Dana digital voltmeter accurate to 0.001 milivolt.

2. Power to Heater

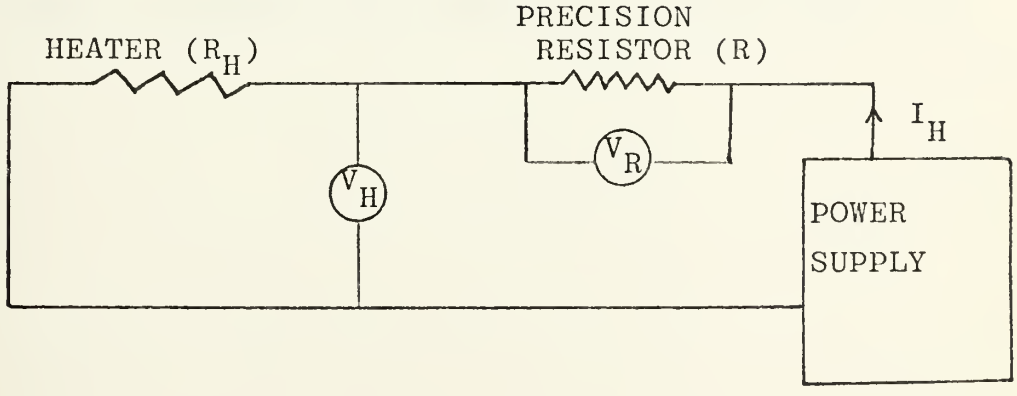

Figure 8. Simple Circuit for Measuring Power to Heater

In order to measure the power input to the heater, a circuit as shown in Figure 8 was constructed. Since R_H is a function of temperature, we should use a more stable resistor (R) (calibrated resistor). With this simple arrangement, a voltage across heater (V_H) and across resistance (V_R) were taken. The current through the circuit could be determined:

$$I_H = VR/R \qquad (3)$$

Knowing R (2.013), V_H and V_R, power was calculated from:

$$P = V_H I_H$$

and from (1):

$$P = V_H(V_R/R) \qquad (4)$$

To get the input power to heater accurately for every run, we needed to measure the values of V_H and V_R from (4) only.

III. EXPERIMENTAL PROCEDURE

A. TEST SURFACE PREPARATION

1. Mirror Finish

A procedure as outlined below was used to prepare each test surface;

The test surface was first sanded with emery paper number 1 and 3. After that, it was washed with detergent and warm water to remove the previous abrasive also a final wash with alcohol.

In order to get a mirror finish surface the test surface was then wet polished on metallurgical wheel covered with velvet. It was impregnated with one micron diamond dust. The test surface was placed face down on the wheel and a low speed of rotation was used. Usually, it took from fourty five minutes to an hour to complete the work. During the work, alcohol was used to wet the surface at all time. After completion of the polishing, the test surface was washed with alcohol again and was dried with a dryer. After work was completed, it was wrapped in special paper to prevent contamination and touching.

2. Cylindrical Cavities

The seven-hole test surface was drilled before the mirror finish. The purpose of making a mirror like surface to insure that the surface conditions were not responsible for the heat-flux of the surface.

Cavities were drilled using Sphinx spirec pivot drill, in 0.015 inch diameter. The cavity depth was controlled by using a fesler gauge on the lathe. A ratio of approximately 2.5 was desired for cavity depth over diameter. So the 0.015 inch holes were drilled to a depth between 0.035 and 0.040 inch.

The locations of seven holes on the test surface was shown in Figure 7: One in the center of the surface and the other six equally spaced on a circle whose center was at the first hole. The holes were spaced 0.165 inch apart.

All of the final measurements were taken to determine the location of the center of the holes for sheathed thermocouples relative to the test surface and the final test diameter was measured. An engineering flat and a scale readable up to 0.0001 inch were used.

B. TEST SURFACE INSTALLATION

Immediately before installation of the seven-hole test surface, it was put in an ultrasonic cleaner for ten minutes then it was washed with distilled water, rinsed with acetone and dried.

C. APPARATUS ASSEMBLY

There are two main parts in the apparatus: 1) the test sections and heater assembly, 2) the tank.

The test heater assembly (section III, B) was rigidly bolted to the phenolic base. After finishing the insulation around the test section and heater assembly, the can was

installed with the insulation inside. A phenolic disc used as the bottom of the tank was fitted to the test section carefully. The level of the test section was adjusted from the bottom base of the assembly by screws. Three long threaded rods were used to secure the upper plate to the phenolic base plate, 120^{o} apart. These three rods also used to adjust the test surface in level with with phenolic bottom plate. A rubber "O" ring was fitted around the test surface and the hole in the bottom plate to prevent leaking. For water, rubber gaskets were used at the bottom and top of the cylindrical plexiglass to make sure that the enclosure did not leak. To secure the top plexiglass plate to the phenolic bottom plate of the tank, six threaded rods were used, 60^{0} apart.

To measure the average bulk temperature of the fluid, four small holes were drilled through the top plexiglass of the tank to insert four pairs of themocouples all wired in series, near the tank wall. One bigger hole was used to pour the fluid into or out of the tank, and was also used as a hole to insert one removable thermocouple used to provide a check on this temperature. It was possible to remove the plexiglass top plate and also the cylindrical wall of the tank without disturbing the test section in order to change the fluid for another run.

It should be noted that the test surface and phenolic bottom plate were cleaned with acetone prior to filling the unit. All other surfaces in contact with the fluid were cleaned with distilled water.

D. FLUID PREPARATION

The test fluid were distilled water and Freon 113. The fluid could be poured into the tank through a one inch diameter hole. A siphon was used to fill the tank.

E. TEST PROCEDURE

1. Temperature

For water, five settings of power input to the heater (10, 20, 30, 40, 50 watts) and for Freon 113 seven settings (1, 2, 3, 4, 5, 6, 7 watts) were used. Data were taken at these settings of power input. At the beginning of each test, a lowest power input was set by the method discussed in section II, C 2. A long time was allowed to elapse until the steady state was reached (usually two to three days for each data point). The same procedure was repeated for each higher power input setting. When we reached the highest power input to the next lower one. When the starting point had reached steady state a complete set of data was obtained for this run.

For each setting, we took data for: 1) themocouples readings in the stainless steel test section, 2) the bulk temperature of the fluid, 3) voltages across heater and calibrated resistor.

Temperature readings were usually taken every hour in the daytime only. When the bulk temperature and the temperature nearest the heater were changed less than half degree per hour, steady state was assumed to have been reached.

2. Determination of Nusselt, Grashof and Rayleigh Numbers

To determine the Nusselt, Grashof and Rayleigh numbers the fluid properties were calculated at the film temperature which is the average of the bulk temperature (T_b) and the test surface temperature (T_s) i.e. $T_f = \frac{T_b+T_s}{2}$. The thermal conductivity of 304 stainless steel (K_{ss}) was calculated using the data from Touloukian [Ref. 17] at the average of the temperature of the two nearest tempermocouples to the test surface i.e. $T_{ss} = \frac{T_0+T_1}{2}$. This corresponds to the average temperature of the length $\Delta x = (x_1-x_0)$.

For each run, the temperature distribution in the stainless steel was found to be linear. For this reason, the test surface temperature could be determined by using linear extrapolation

$$T = B_1 x + B_2 \tag{5}$$

Using the two nearest themocouples readings to the test surface, substituting into equation (5) and note that, at surface, x = 0, thus:

$$T_{surface} = B_2 \tag{6}$$

and

$$B_1 \ \alpha \text{ heat flux at surface} = \frac{\Delta T}{\Delta x} = \frac{(T_1 - T_0)}{(x_1 - x_0)} \tag{7}$$

A simple energy balance at the surface, using Fourier's Law of Conduction yields:

$$K_{ss} \frac{\delta T_{ss}}{\delta x} = h\ (T_{surface} - T_{bulk}) \tag{8}$$

The Nusselt number was obtained from the definition:

$$Nu = \frac{hD}{K_f} \tag{9}$$

and

$$Q = hA(T_s - T_b) = K_{ss}\ A\ (\frac{\Delta T}{\Delta x}) \tag{10}$$

or

$$h = \frac{Q}{A(T_s - T_b)} = \frac{Q}{A(B_2 - T_4)} \tag{11}$$

From (9), $$Nu = \frac{QD}{A(B_2 - T_4)Kf} \tag{12}$$

From (10) and (7), we thus obtained:

$$Nu = \frac{B_1 D K_{ss}}{K_f\ (B_2 - T_4)} \tag{13}$$

The Grashof number was calculated using the diameter of the heated test surface as the characteristic length:

$$Gr = \frac{g\beta\ D^3\ (T_s - T_b)}{\nu^2} \tag{14}$$

or

$$Gr = \frac{g\beta}{\nu^2}\ D^3\ (B_2 - T_4) \tag{15}$$

The Rayleigh number is the product of the Grashof number and Praudlt number:

$$Ra = Gr \cdot Pr \tag{16}$$

A simple calculation for water is contained in Appendix B, 1 and for Freon in Appendix B, 2.

If we use the heigh or radius of the tank as a characteristic length then the Grashof number becomes:

$$Gr_H = Gr_R = \left(\frac{g\beta}{\nu^2}\right) H^3 (B_2 - T_4) \tag{17}$$

Since the test section diameter was chosen to be one fifth the heigh of the tank thus we have the relation for Grashof numbers:

$$Gr_H = Gr_R = 125\ Gr \tag{18}$$

TABLE I

UNCERTAINTIES IN THE EXPERIMENT (For Water)

Power input Settings (Watts)	Percent Uncertainty		
	Nusselt Number	Grashof Number	Rayleigh Number
11.12	6	6	6
20.12	4	4	4
30.93	3	8	8
40.93	3	2	3
50.54	3	1	2

TABLE II

UNCERTAINTIES IN THE EXPERIMENT (Freon, Seven-Hole)

Power input Settings (Watts)	Percent Uncertainty		
	Nusselt Number	Grashof Number	Rayleigh Number
1.16	8	8	7
2.13	9	8	8
3.13	7	9	9
4.14	8	9	8
5.13	8	8	9
6.10	8	7	9
7.27	7	8	7

TABLE III

UNCERTAINTIES IN THE EXPERIMENT (Freon, Blank)

Power input Settings (Watts)	Percent Uncertainty		
	Nusselt Number	Grashof Number	Rayleigh Number
1.12	7	6	6
2.13	8	8	6
3.13	7	6	6
4.13	6	7	7
5.28	7	8	7
6.51	7	7	6
7.26	6	5	7

IV. RESULTS AND DISCUSSION

This investigation covers a range of Grashof number (based on test surface diameter) from 1×10^6 to 16×10^6 for water with seven-hole test section and for Freon 113 a range from 4×10^6 to 25×10^6 with seven-hole test section and from 3×10^6 to 23×10^6 with blank test section. A range of Prandlt number from 2.58 to 4.65 (with seven-hole test section) for water and for Freon 113, at a range from 7.65 to 8.84 (seven-hole test section) and from 7.52 to 8.38 with blank test section. A summary of the results can be found from Table IV, V and VI.

Two different surfaces were tested and twenty-nine runs were made. The natural convection data points were plotted in Figure 9 through 16 and approximated by straight lines.

In section II, C the bulk temperature of fluid was calculated. To reach steady state for each input setting, a minimum of twenty-four hours was needed. Figure 9 is a log-log plot of the Nusselt versus the Grashof number for water with seven-hole test surface. For this plot, a very good agreement between the heating and cooling phase of Nusselt and Grashof number (based on test surface diameter) was obtained.

A brief discussion of the result of water with seven-hole test section as compared with the work of O'Connor with blank test section [Ref. 3] is needed to have some

conclusions on the effect(s) of drilled cavities on heat transfer (ref to Figures 9, 10). The log-log plot of the Nusselt number vs Grashof number (based on test section diameter) was approximated by a straight line which has the same slope as that of the least square fit of O'Connor's results but with a lower intercept. The work of Mr. O'Connor was discussed in the introduction of this experiment. Also, a comparison of the result with that of Torrance [Ref. 11] is illustrated in Figure 9. A Prandlt number of 0.7 (air) was assumed by Torrance and the Grashof number was based on cylinder height and list spot temperature.

For Freon 113 with seven-hole test section, the approximate straight line is lower than that of the blank test section but the slopes are the same in both cases. A log-log plot of the Nusselt number versus the Grashof number for seven-hole test section and blank test section is shown in Figure 15.

Some of the data points were taken during the cooling phase (when power inputs were decreased). These points were denoted by << ' >> in the Table. For cooling phase at a power input setting, to compare with that of the heating phase at the same Grashof number the Nusslet number is a little bit lower. For Nusselt number versus Rayleigh number, the data for cooling phase (correspond to the same power input setting) has almost the same Rayleigh number with the corresponding point in the upward phase but the Nusselt number is lower (for the case of water with seven-hole test

section, Figure 9); for Freon 113 the corresponding point in the cooling phase has almost the same Ra but the Nu is lower. The Nusselt number vs Rayleigh number (log-log plot) is plotted in Figure 10 for water with seven-hole test section to compare with the result of O'Connor [Ref. 3]. Figure 12 is a plot for the case of Freon 113.

The heat transfer correlation which results from this experimental data is:

$Nu = 0.38\ (Ra)^{0.29}$ for water with seven-hole test section

$Nu = 0.48\ (Ra)^{0.30}$ for Freon with seven-hole test section

and $Nu = 0.53\ (Ra)^{0.30}$ for Freon with blank test section.

Torrance [Ref. 12] in his numerical solution, assumed a uniform fluid bulk temperature and in his experimental work, used an average of the container wall temperature and the floor temperature. He obtained a good agreement between his experimental and numerical method. In this thesis, an average bulk temperature was used (automatically obtained from the reading of eight thermocouples inserted in the fluid).

TABLE IV

SUMMARY OF RESULTS FOR WATER (With 7-Hole Test Section)

Input(Watt)	Ts	T_f	Nu	Log(Nu)	$Grx10^{-6}$	Log(Gr)	$Rax10^{-6}$	Log(Ra)
11.12	110.15	97.88	34.49	1.55	1.13	6.05	5.25	6.72
20.12	132.55	114.34	45.05	1.65	3.18	6.50	12.75	7.11
30.93	156.09	131,31	50.48	1.70	6.57	6.82	22.4	7.35
40.02	176.00	144.82	50.14	1.70	10.52	7.02	30.72	7.49
50.54	194.09	159.15	55.87	1.75	16.31	7.21	42.08	7.62
50.55'	194.86	159.32	55.00	1.74	16.66	7.22	42.98	7.63
40.19'	176.28	144.65	49.79	1.70	10.65	7.03	31.20	7.49
30.91'	156.41	130.90	48.41	1.68	6.71	6.83	22.94	7.36
20.21'	133.88	115.02	43.58	1.64	3.36	6.53	13.38	7.13
11.17'	111.86	99.50	37.02	1.57	1.19	6.08	5.41	6.73

': indicates cooling phase

TABLE V

SUMMARY OF RESULTS FOR FREON (With 7-Hole Test Section)

Input(Watt)	Ts	T_t	Nu	Log(Nu)	$Grx10^{-6}$	Log(Gr)	$Rax10^{-6}$	Log(Ra)
1.16	83.27	79.72	96.79	1.986	3.81	6.580	33.68	7.527
2.13	88.63	82.57	105.09	2.022	7.16	6.855	59.50	7.775
3.13	94.82	86.46	110.80	2.045	9.95	7.000	81.29	7.910
4.14	99,24	88.82	119.29	2.077	12.75	7.106	103.02	8.013
5.13	104.20	91.84	125.24	2.097	16.22	7.210	129,43	8.110
6.10	111.99	97.19	132.52	2.123	20.80	7.310	161.82	8.209
7.27	116.67	99.84	139.69	2.145	24.49	7.289	187.35	8.273
5.12'	104.20	91.84	125.24	2.097	16.22	7.210	129.43	8.110
4.13'	97.96	104.59	118.99	2.075	12.45	7.095	101,09	8.005
3.14'	94.12	99.00	108.88	2.037	9.97	6.99	81.85	7.910
2.12'	88.10	82.05	100.14	2.000	6.82	6.834	52.31	7.719
1.13'	82.76	79.27	97.70	1.981	3.73	6.572	31.52	7.498

': indicates cooling phase

TABLE VI

SUMMARY OF RESULTS FOR FREON (With Blank Test Section)

Input(Watt)	Ts	T_f	Nu	Log(Nu)	$Grx10^{-6}$	Log(Gr)	$Rax10^{-6}$	Log(ra)
1.12	83.70	80.63	98.73	1.994	3.41	6.533	28.58	7.456
2.13	88.06	82.49	111.57	2.048	6.32	6.801	52.58	7.721
3.13	93.76	86.00	120.38	2.081	9.19	6.963	74.62	7.873
4.13	98.61	88.86	131.93	2.120	11.05	7.077	95.62	7.981
5.28	104.36	92.33	137.16	2.137	15.88	7.200	124.02	8.094
6.51	108.58	94.79	148.00	2.170	18.80	7.274	144.92	8.161
7.26	114.11	98.25	151.58	2.181	22.66	7.355	170.04	8.231

V. CONCLUSIONS AND RECOMMENDATIONS

The results lead to the following conclusions:

1. Cylindrical drilled cavities affect the natural convection heat-transfer of water and Freon 113: the line of log-long plot of the Nusselt number vs Grashof number and Rayleigh number with seven-hole test section is lower than that of O'Connor (with blank test section) for water, but the slope is almost the same.

2. The heat transfer line in the log-log plot of the Nusselt number versus Grashof number and Rayleigh number for Freon 113 is higher than that of water with the same test section.

3. For water with seven-hole test section, a correlation which results from this experimental data is:

$$Nu = 0.38(Ra)^{0.29}$$ for water and $$Nu = 0.48(Ra)^{0.30}$$

for Freon 113 with seven-hole test section and

$$Nu = 0.53(Ra)^{0.30}$$

for Freon 113 with blank test section

The following recommendations are made for future work:

1. Continue the present studies with different size and number of cavities (say one, thirteen, and ninety six cavities) and compare the results with this experimental work.

2. Using a power setting of at least eight watts for the case of Freon 113 to get a boiling curve and the result would be compared to that of Mr. Moulson [Ref. 15].

3. Using the same test sections but different fluids to investigate the effects of changing fluid.

4. Study the effects of different cavity geometeries (say cylindrical, conical, reentrant).

5. Find a method to get the bubbles out of the tank if the power input is greater than 40 watts in case of water to get a good result on heat transfer.

6. Rework this experimental stady with the flow visualization technique and compare the results with the results of this study.

Figure 9

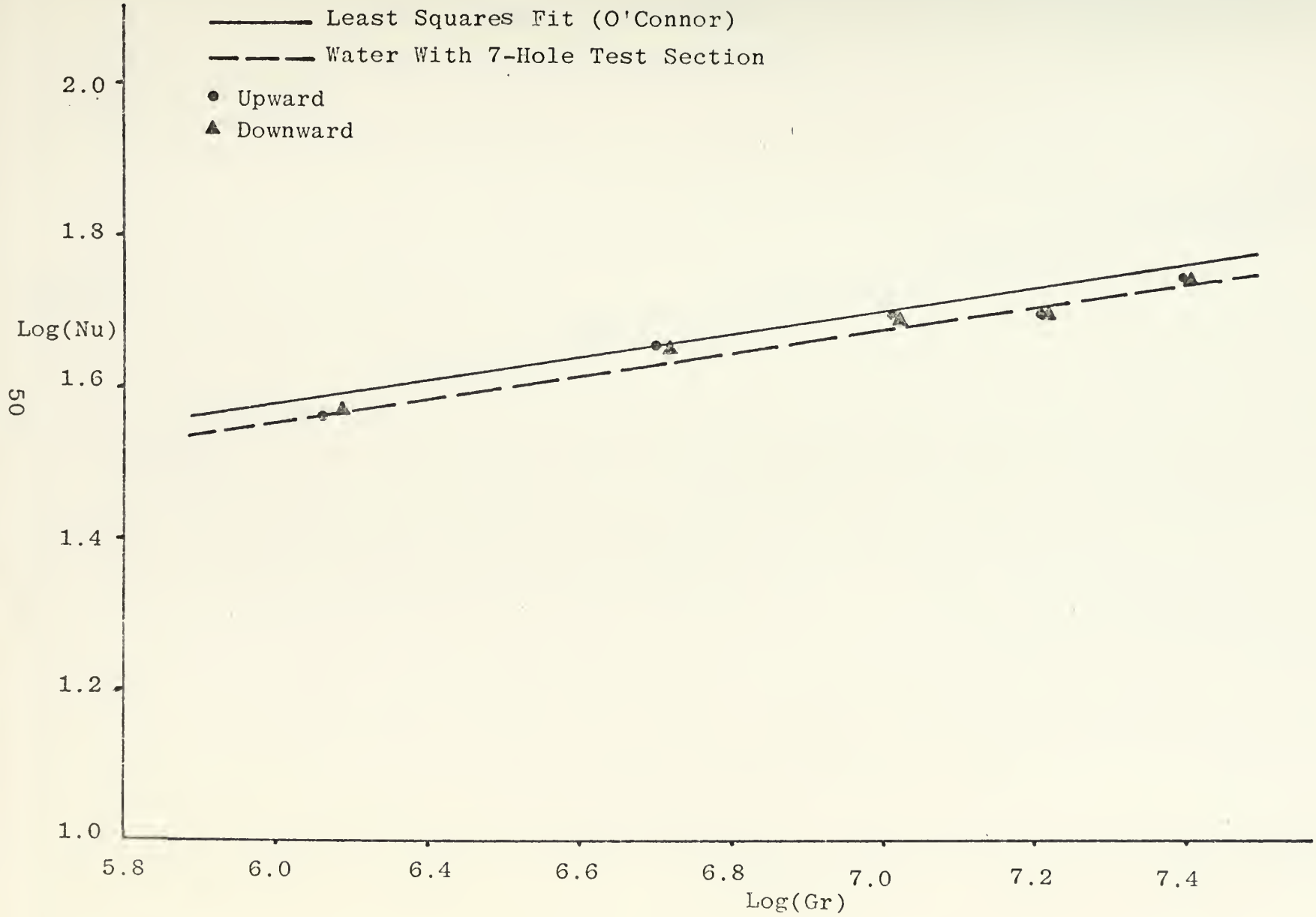
Least Squares Fit (O'Connor)
Water With 7-Hole Test Section
Upward
Downward
2.0
1.8
1.6
1.4
1.2
1.0
Log(Nu)
50
5.8
6.0
6.4
6.6
6.8
7.0
7.2
7.4
Log(Gr)

Figure 10

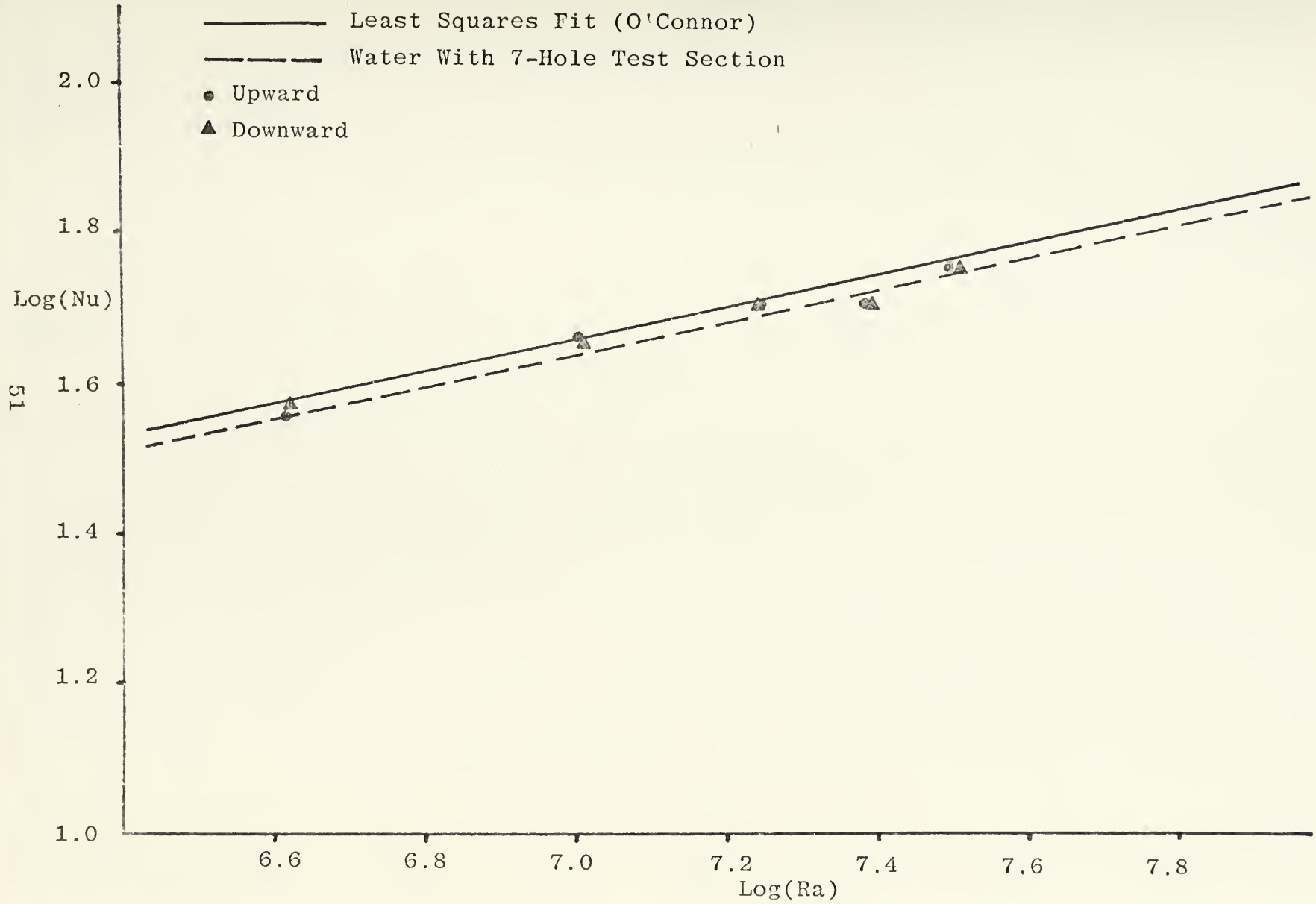
Least Squares Fit (O'Connor)
Water With 7-Hole Test Section
Upward
Downward
2.0
1.8
1.6
1.4
1.2
1.0
Log(Nu)
6.6
6.8
7.0
7.2
7.4
7.6
7.8
Log(Ra)

Figure 11

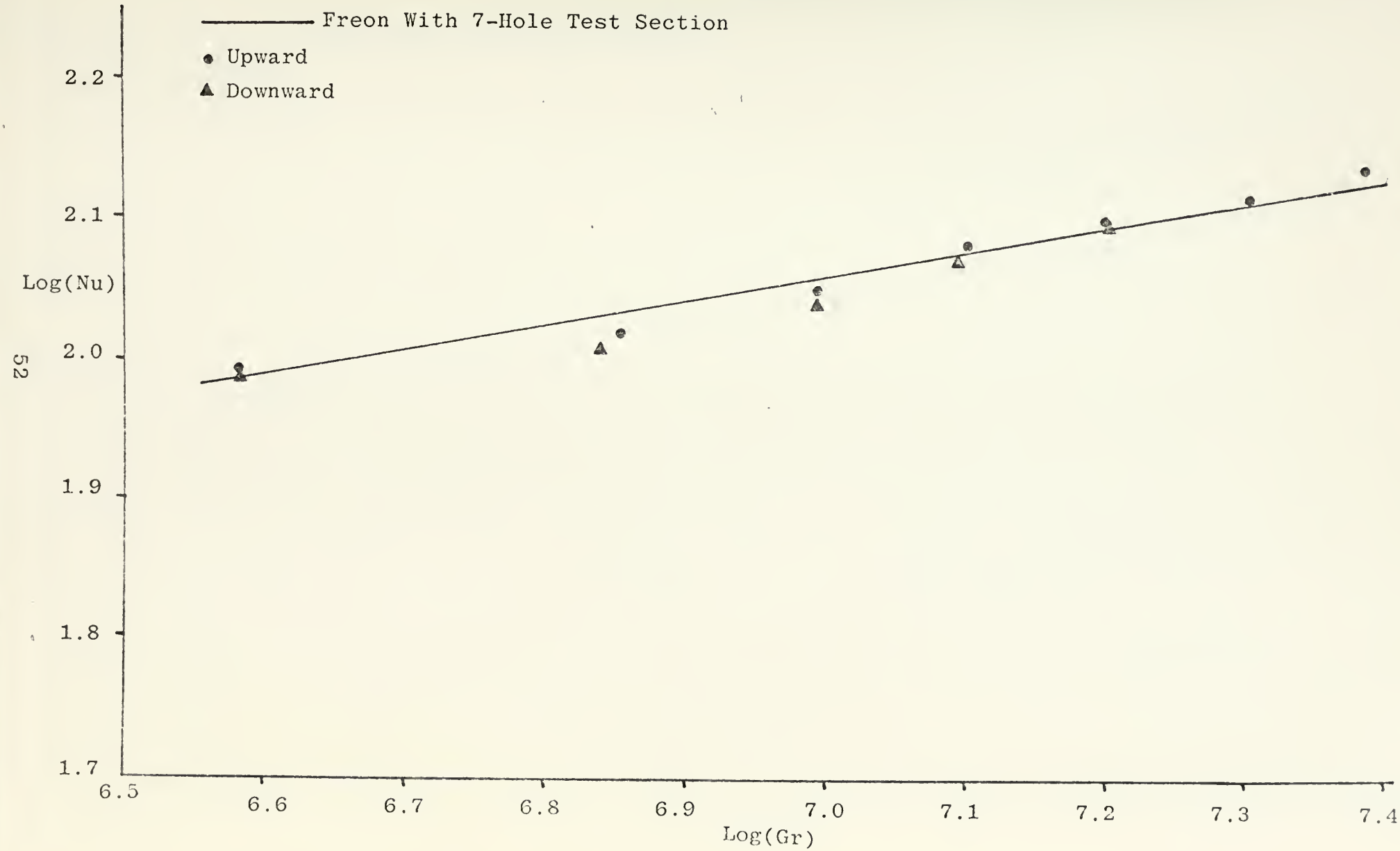
Freon With 7-Hole Test Section
Upward
Downward
2.2
2.1
Log(Nu)
2.0
1.9
1.8
1.7
6.5
6.6
6.7
6.8
6.9
7.0
7.1
7.2
7.3
7.4
Log(Gr)

Figure 12

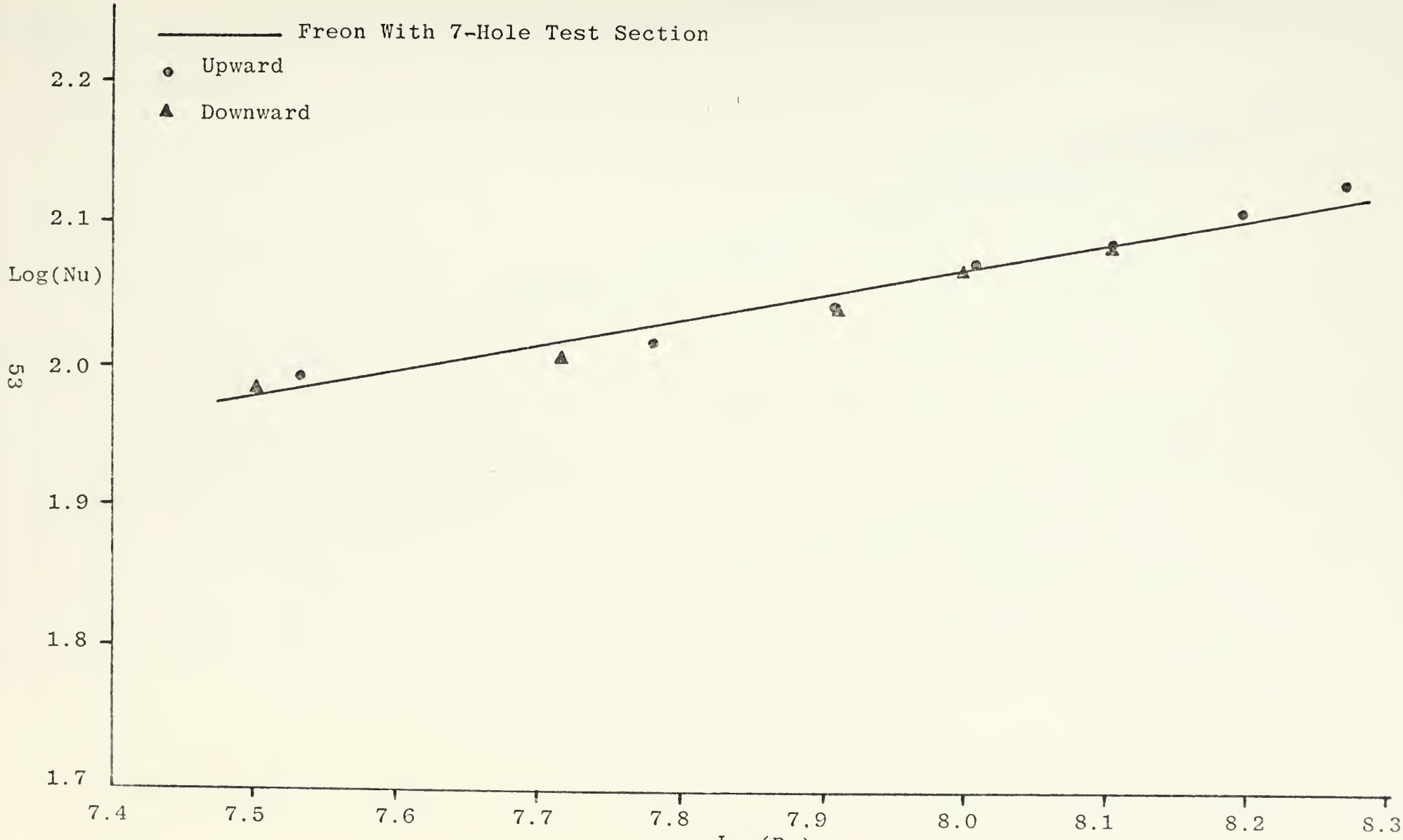
Freon With 7-Hole Test Section
Upward
Downward
2.2
2.1
Log(Nu)
2.0
1.9
1.8
1.7
7.4
7.5
7.6
7.7
7.8
7.9
8.0
8.1
8.2
8.3
Log(Ra)

Figure 13

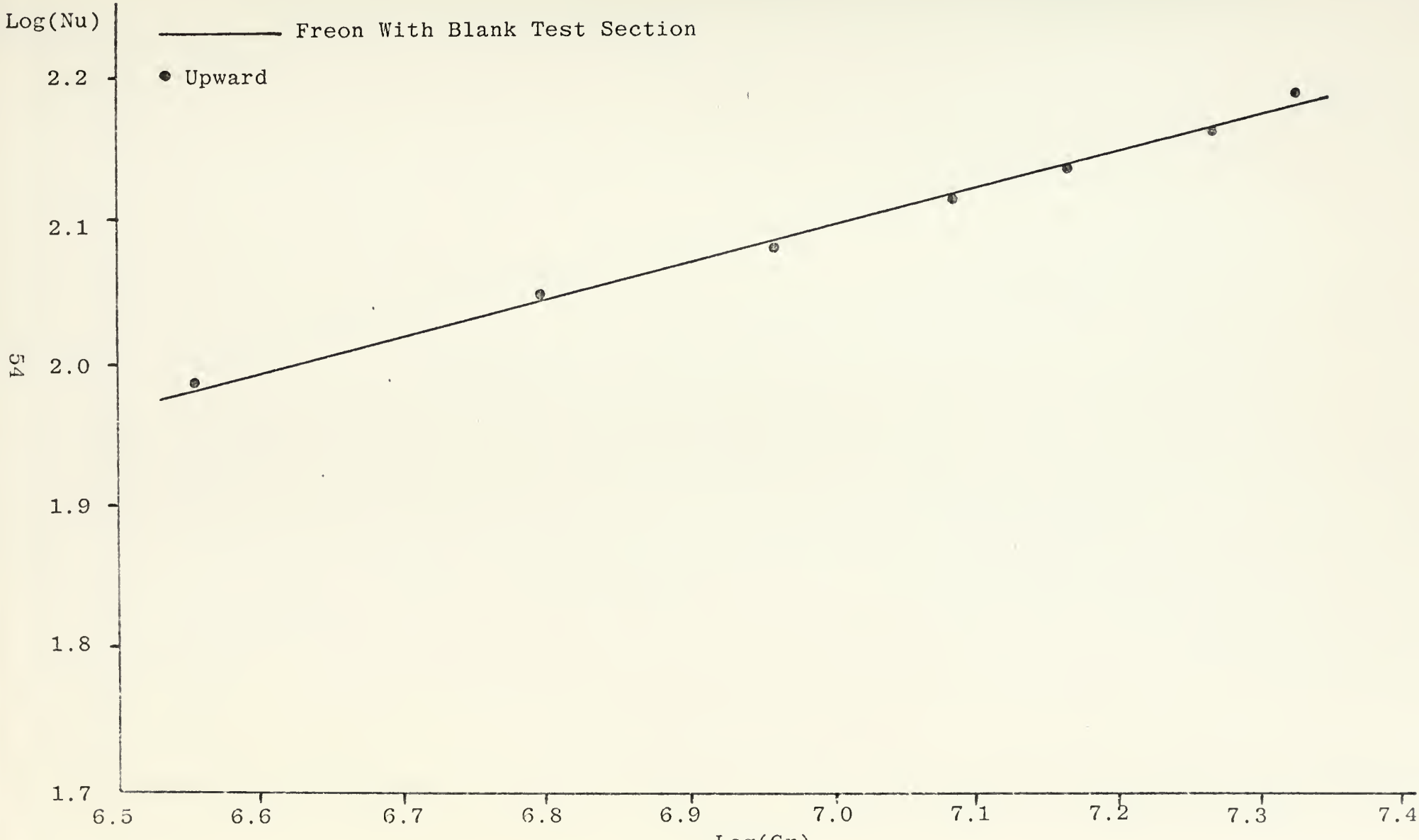
Log(Nu)
Freon With Blank Test Section
Upward
2.2
2.1
2.0
1.9
1.8
1.7
6.5
6.6
6.7
6.8
6.9
7.0
7.1
7.2
7.3
7.4
Log(Gr)

Figure 14

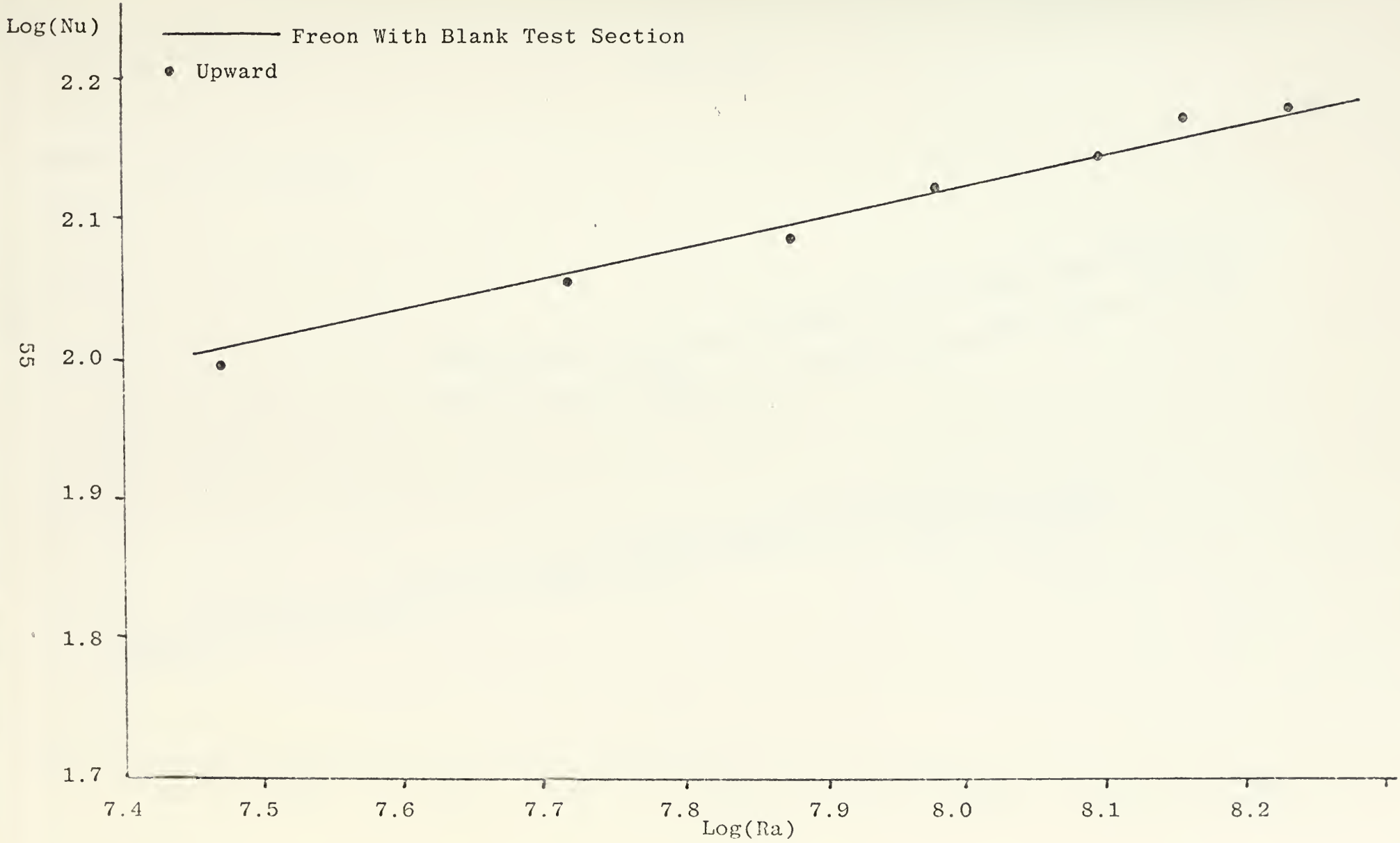
Log(Nu)
Freon With Blank Test Section
Upward
2.2
2.1
2.0
1.9
1.8
1.7
7.4
7.5
7.6
7.7
7.8
7.9
8.0
8.1
8.2
Log(Ra)

Figure 15

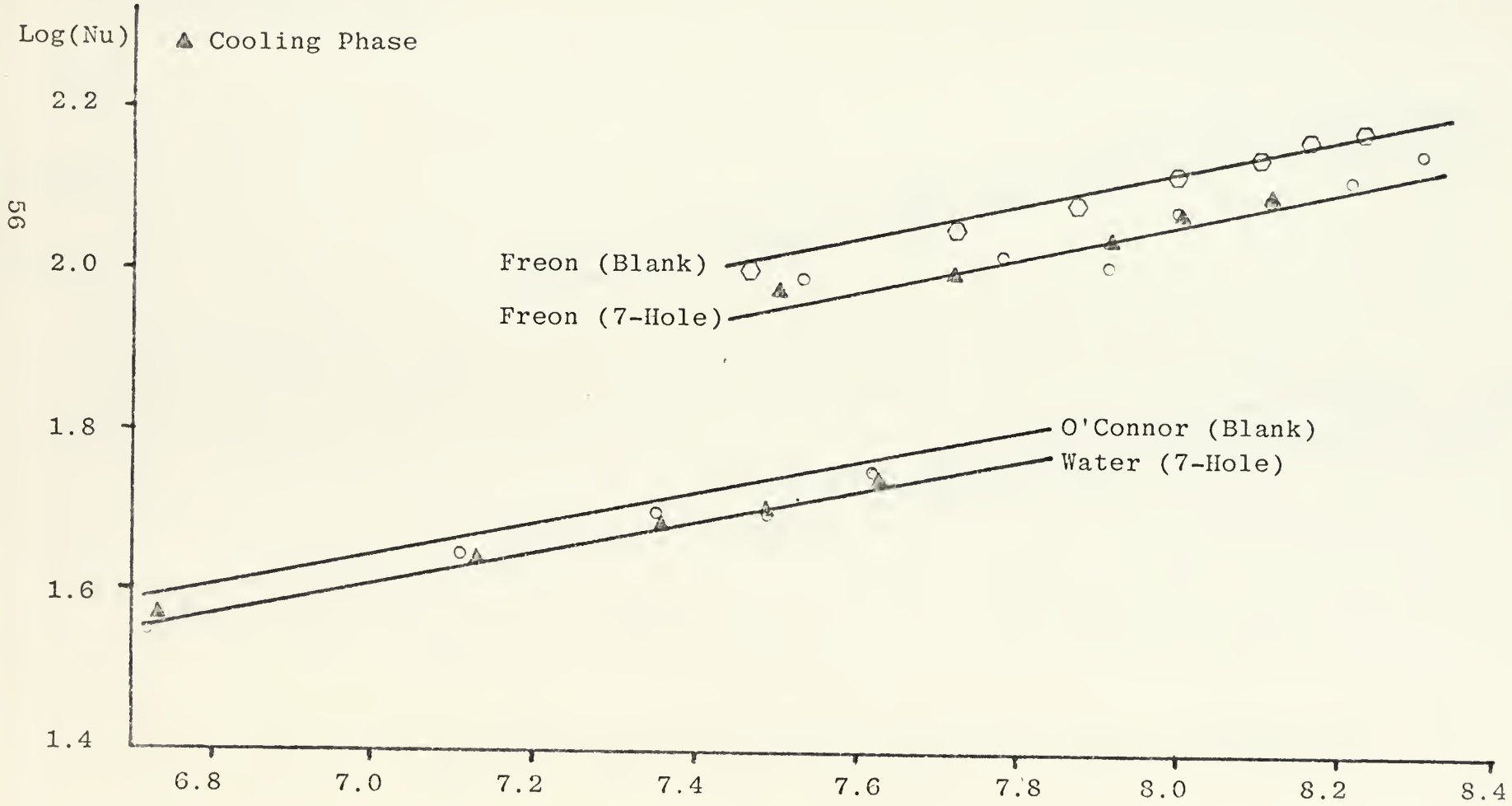
Log(Nu)
Cooling Phase
2.2
2.0
1.8
1.6
1.4
Re
Freon (Blank)
Freon (7-Hole)
O'Connor (Blank)
Water (7-Hole)
6.8
7.0
7.2
7.4
7.6
7.8
8.0
8.2
8.4

Figure 16

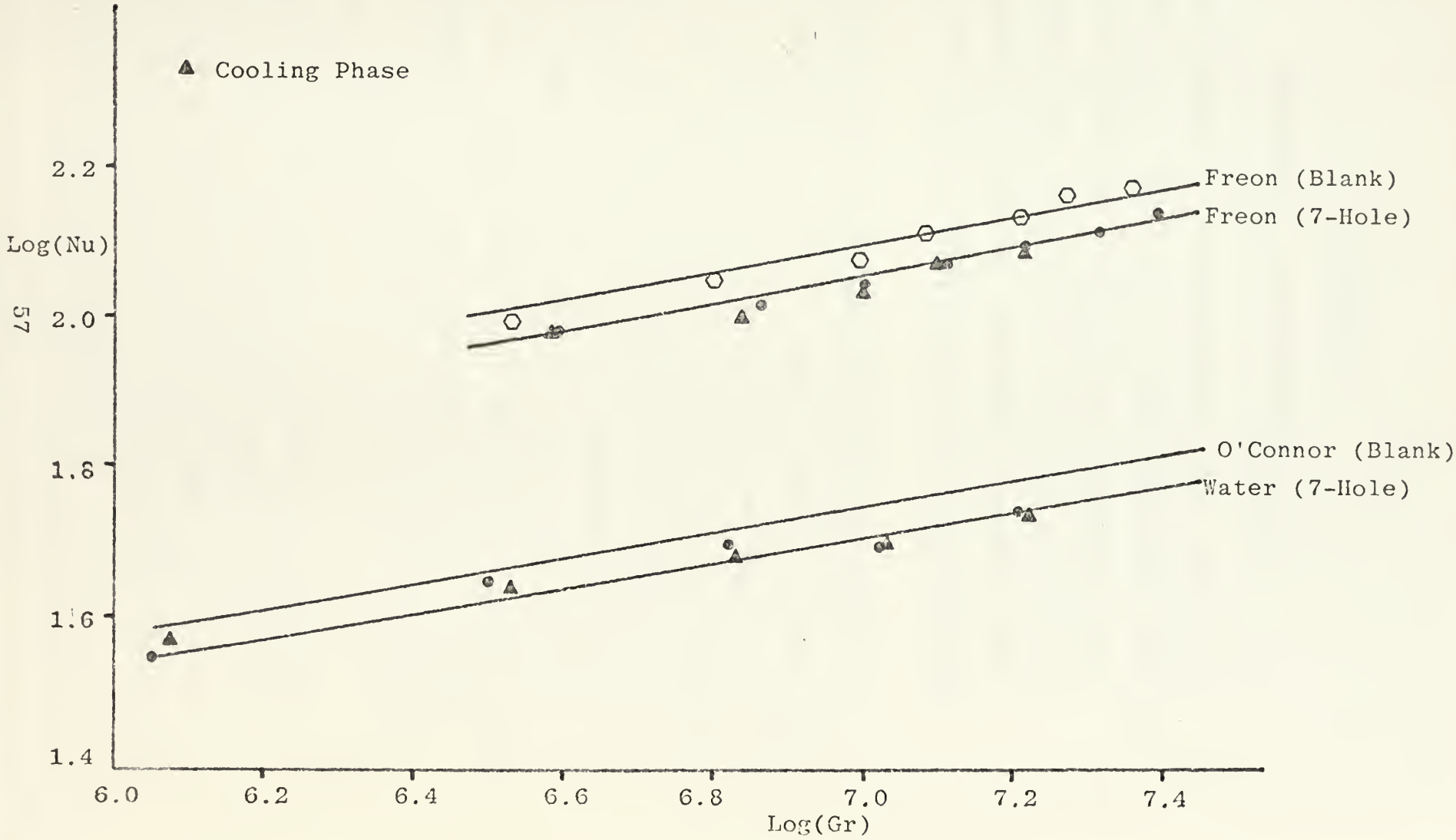
Cooling Phase
Freon (Blank)
Freon (7-Hole)
O'Connor (Blank)
Water (7-Hole)
Log(Nu)
Log(Gr)
2.2
2.0
1.8
1.6
1.4
6.0
6.2
6.4
6.6
6.8
7.0
7.2
7.4

APPENDIX A

THERMOCOUPLE CALIBRATION PROCEDURE

The calibration of the sheathed and bulk temperature thermocouples was a major part of this experiment since all the results and discussion based on the accuracy of the determination of the test surface and fluid temperatures. All the wiring and recording instruments would be used in the experiment were not changed after the calibration was completed.

A Rosemount type of calibration system was used with a constant temperature oil path. The ice junction thermocouple (sealed in a glass tube, filled with oil) was placed in a stainless steel dewar filled with ice water and circulated with a pump. The nine bulk temperature thermocouples and the four sheathed thermocouples were suspended about three about three inches into the oil bath. The calibration was conducted over a range from $80^{0}F$ to $324^{o}F$ and a maximum error for the thermometer for this temperature range was $0.005^{o}F$. A Platinum Resistance thermometer with a commutation bridge was used as a standard.

A comparison of the calibration results with standard thermocouple tables: for the sheathed thermocouples the result was good with deviation from the table values in a range from -0.012 mv to +0.005 mv and for the bulk temperature in a range from -0.009 mv to +0.001 mv.

The above results led us to use the standard tables with an uncertainty in the sheathed thermocouples reading of $0.5^{o}F$ and $0.5^{o}F$ in the bulk temperature reading.

APPENDIX B

SAMPLE CALCULATIONS

I. FOR WATER

These calculation are for data recorded on 20 December 1974 for an input of 11.12 watts and with seven-hole test surface.

1. Determination of the Surface Temperature

To determine the temperature of the test surface a graphical method was used. A plot of the temperature versus the thermocouple distance from the test surface was made for each run (corresponding to a proper setting of power input), as shown in Figure 17 using the two nearest sheathed thermocouples to the test surface. Using a linear extrapolation to obtain the surface temperature an error within $0.5^{o}F$ could be obtained.

2. Calculation of the Nusselt Number

Using the equation (13) of section III, E2 to calculate the Nusselt number:

$$Nu = \frac{B_1 DK_{ss}}{K_f(B_2 - T_4)} \qquad \text{(II-A)}$$

The value of K_{ss} was obtained based on an average temperature of the cylinder over the length Δx using the two nearest temperatures to the test surface in the stainless steel cylinder. The values of Kss were obtained using the

Figure 17

DETERMINATION OF SURFACE TEMPERATURE

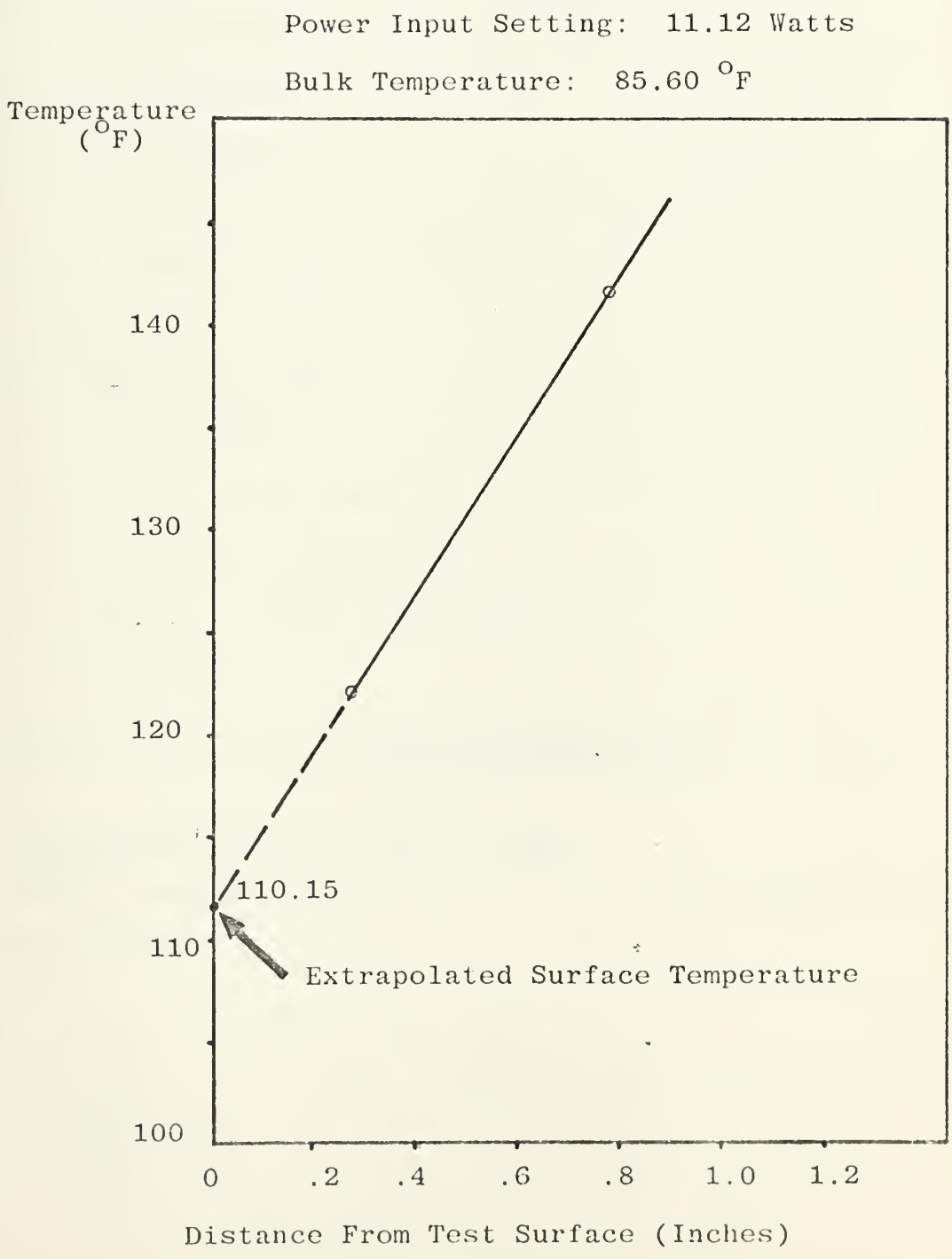

data from Touloukian [Ref, 17], Fluid properties were evaluated at the film temperature i.e. $T_f = \frac{T_s + T_b}{2}$ (section III, E2) using the data from the Table VI, Appendix C, from Kreith [Ref. 18]. For 11.12 Watts input setting, the following were obtained:

$T_0 = 120.04^{\circ}F$

$T_1 = 139.54^{\circ}F$

$T_4 = 85.00^{\circ}F$

$D = 0.07458$ ft.

$\Delta x = 0.04183$ ft.

$B_1 = 566.14$ Btu/hr-ft^2

$B_2 = 110.15^{\circ}F$

$Tss = 129.79^{\circ}F$

$T_f = 97.88^{\circ}F$

$Kss = 9.099$ Btu/hr-ft-$^{\circ}F$

$K_f = .363$ Btu/hr-ft-$^{\circ}F$

$g\beta/_{\nu}2 = 111.000 \times 10^6$ 1/ft^3-or

$Pr = 4.65$

and from (II-A) $Nu = \frac{(466.14)(0.07458)(9.099)}{.363(110.15-85.60)} = 35.49$

3. Calculation of the Grashof Number

Using equation (15) of section III, E2 to calculate the Grashof number:

$$Gr = (g\beta/_{\nu}2)\, D^3\, (B_2 - T_4) \qquad (15)$$

The values $g\beta/_{\nu}2$ were calculated from Appendix C, from Kreith [Ref. 18].

For 11.12 watts input setting, the Grashof number is;

$$Gr = 111.00 \times 10^6 \ (0.07458)^3(110.15 - 85.60) = 1.13 \times 10^6$$

4. Calculation of the Rayleigh Number

Using equation (16) of section III, E2, the Rayleigh number is the product of the Grashof number and Prandlt number:

$$Ra = Gr \cdot Pr \qquad (19)$$

using (12) the Rayleigh number is

$$R_a = 1.13 \times 10^6(4.65) = 5.25 \times 10^6$$

II. FOR FREON 113

The following is a sample calculation of the Nusselt, Grashof and Rayleigh numbers for data recorded on 19 March 1975 for 1.16 watt of power input setting and with seven-hole test surface.

1. Determination of the Surface Temperature

Using the same method in I-1, the test surface temperature was obtained in Figure 18.

2. Calculation of the Nusselt Number

Using the quation (II-1) of section III, E2 to calculate the Nusselt number:

$$Nu = \frac{(B_1)(D)(K_{ss})}{K_f(B_2 - T_4)} \qquad (II\text{-}1)$$

The values of K_{ss} were obtained using the data from Touloukian [Ref. 17]. Fluid properties were evaluated at the film temperature $T_f = \frac{T_s + T_b}{2}$ (section III, E2) using the

Figure 18

DETERMINATION OF SURFACE TEMPERATURE

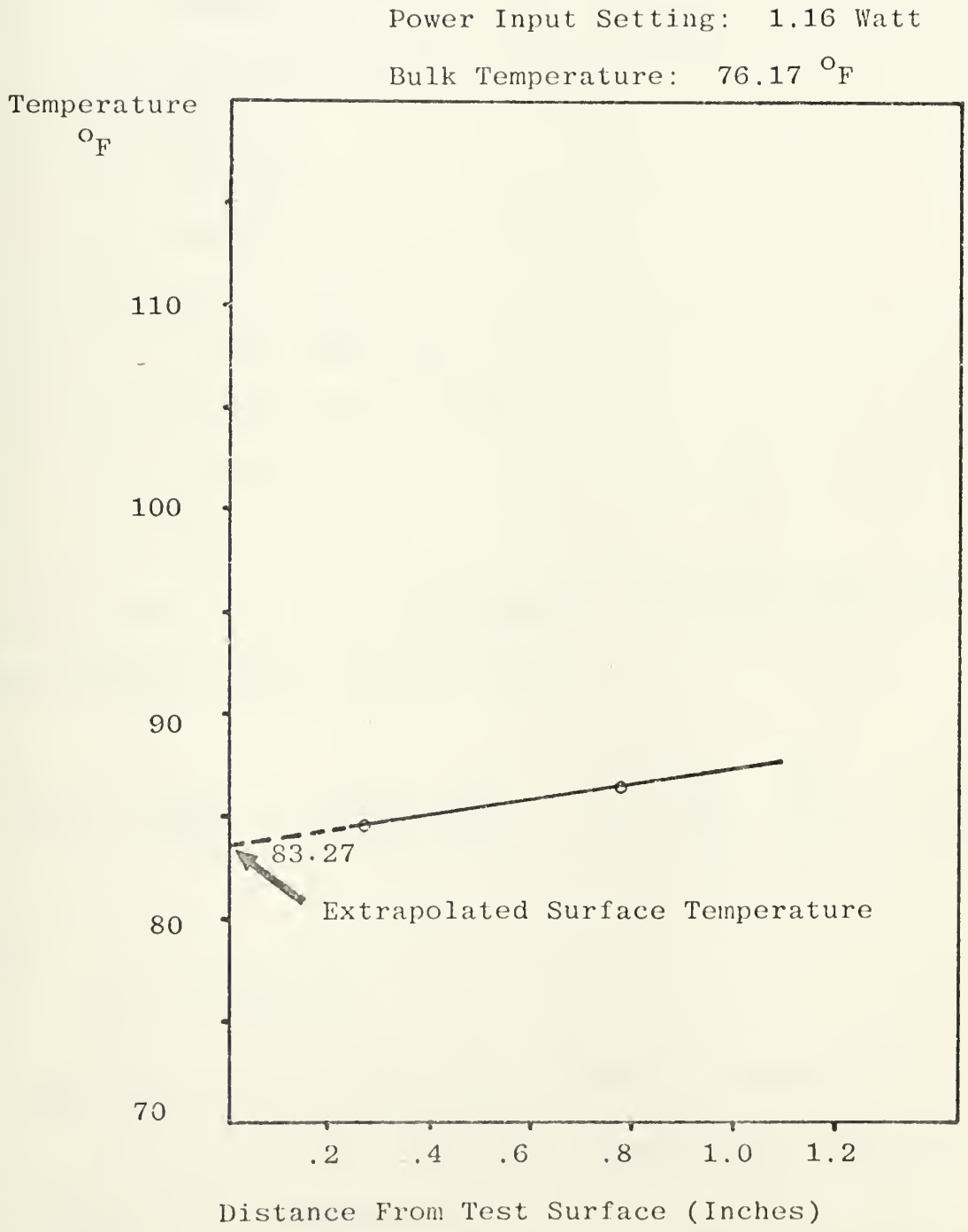

data from Table II and Table 13 from Thermophysical Properties of Refrigerant 113 [Ref. 19]. For 1.16 watt of power input setting, the following were obtained:

$T_0 = 84.23^{\circ}F$

$T_1 = 86.12^{\circ}F$

$T_4 = 76.17^{\circ}F$

$D = 0.07458$ ft.

$B_1 = 45.18$ Btu/hr-ft^2

$B_2 = 83.27^{\circ}F$

$Tss = 85.17^{\circ}F$

$T_f - 79.72^{\circ}F$

$Kss = 8.81$ Btu/hr-ft-$^{\circ}F$

$\mu = 1.592$ lbm/ft-hr

$K_f = 0.0432$ Btu/hr-ft-$^{\circ}F$

$Cp = .229$ Btu/lbm-$^{\circ}F$

$\rho = 97.47$ lbm/ft^3

The values of β were calculated by definition from the thermo-dynamic properties [Ref. 20].

$$\beta = -\frac{1}{\rho}\left(\frac{d\rho}{dT}\right)_{\rho} = -\frac{1}{\rho}\left(\frac{\rho 2 - \rho 1}{T_2 - T_1}\right)_{\rho} = -v_f \frac{\frac{1}{v_{f2}} - \frac{1}{v_{f1}}}{T_2 - T_1} \qquad (20)$$

with

$$v_f = \frac{v_{f2} + v_{f1}}{2}$$

For 1.16 watt of power input setting, we have:

$\beta = 8.28 \times 10^{-4}$ $1/^{\circ}R$ using a temperature difference $T_2 - T_1 = 10^{\circ}F$ in equation (20).

The Prandlt numbers were calculated by definition;

$$Pr = \nu/\alpha = \frac{\mu}{\rho} \quad \frac{\rho\ Cp}{K_f} = \frac{\mu\ Cp}{K_f} \qquad (21)$$

Using (21), the Prandlt number for 1.16 watt of power input setting is:

$$Pr = \frac{(1.592)(.229)}{0.0432} = 8.84$$

Using equation (9), we have:

$$Nu = \frac{(45.18)(0.07458)(8.81)}{0.0432\ (83.27 - 76.17)} = 96.79$$

3. Calculation of the Grashof Number

Using equation (15) of section III, E2 to calculate the Grashof number

$$Gr = (g\beta/_{\nu}2)\ D^3\ (B_2 - T_4) \qquad (22)$$

Using the units stated in the table of the thermophysical properties of Freon 113 [Ref. 21] and D = 0.07458 ft, we have:

$$Gr = (173135.52)(\beta)(\rho/\mu)^2(B_2 - T_4) \qquad (23)$$

Using this equation, the Grashof number is:

$$Gr = (173235.52)(8.28 \times 10^{-4})(\frac{97.47}{1.592})^2 (83.27 - 76.17)$$

$$Gr = (3.81) \times 10^6$$

4. Calculation of the Rayleigh Number

Using equation (12) of section III, E2, the Rayleigh number is the product of the Grashof number and Prandlt number:

$$Ra = Gr \cdot Pr \tag{24}$$

Thus,

$$Ra = (3.81 \times 10^6)(8.84) = 33.68 \times 10^6$$

APPENDIX C

UNCERTAINTY ANALYSIS

The method proposed by Kline and Mc Clintock [Ref. 21] to obtain the uncertainties was used in this experimental work. The following table is a summary of these quantities including assumptions and approximations to get an estimate of the uncertainties for each variable.

TABLE VII

Uncertainty of Variables

Variable	Basis for Value	Uncertainty (U)
Ts	dictated by scale of graphical method	$0.5^{o}F$
T_b	thermocouple calibration	$0.5^{o}F$
T_0 and T_1	thermocouple calibration	$0.5^{o}F$
$K_f(H_2O)$	assumption based on table values [Ref. 18]	0.001 Btu/hr-ft-^{o}F
Kss(304 s.s.)	assumption based on table values [Ref. 17]	5% Btu/hr-ft-^{o}F
K_f(Freon 113)	assumption based on table values [Ref. 19]	5% Btu/hr-ft-^{o}F
$g\beta/\nu 2(H_2O)$	assumption based on table values [Ref. 18]	0.01 $1/ft^3$-^{o}F
$g\beta/\nu 2$ (Freon 113)	assumption based on table values [Ref. 19]	0.01 $1/ft^3$-^{o}F
δx	accuracy of measurement	0.42×10^{-3} ft
D	accuracy of measurement	0.20×10^{-3} ft

$Pr(H_2O)$	assumption based on table values [Ref. 18]	5%
μ(Freon 113)	assumption based on table values [Ref. 19]	0.002 lbm/ft-hr
Cp(Freon 113)	assumption based on table values [Ref. 19]	0.001 Btu/lbm-^oF
β(Freon 113)	assumption based on table values [Ref. 19]	0.1 x 10^{-4} $1/^oR$
ρ(Freon 113)	assumption based on table values [Ref. 19]	0.01 lbm/ft^3

Using the second-power equation of Kline and Mc Clintock Ref. 21 to calculate the uncertainties in the values obtained experimentally.

Let U_{Ts} = uncertainty in Ts

U_{Tb} = uncertainty in T_b

then, $$U_{\delta T} = U_{Ts - Tb} = \left[(U_{Ts})^2 + (U_{Tb})^2 \right]^{\frac{1}{2}}$$

$$= \left[(0.5)^2 + (0.5)^2 \right]^{\frac{1}{2}} = .707^oF \qquad (25)$$

and $$U_{\delta Tss} = U_{T_1 - T_0} = \left[(U_{T_1})^2 + (U_{T_0})^2 \right]^{\frac{1}{2}}$$

$$= \left[(0.5)^2 + (0.5)^2 \right]^{\frac{1}{2}} = 0.707^oF \qquad (26)$$

From equation (8), section III, E2, we have

$$h = \frac{K_{ss}}{\delta T} \quad \frac{\delta T_{ss}}{\delta x}$$

and using the second-power equation of Kline and Mc Clintock [Ref. 21] we have:

$$\frac{Uh}{h} = \left[\left[\frac{U_{Kss}}{Kss}\right]^2 + \left[\frac{U\delta T_{ss}}{\delta T_{ss}}\right]^2 + \left[\frac{U\delta x}{\delta x}\right]^2 + \left[\frac{U_{\delta T}}{\delta T}\right]^2 \right]^{\frac{1}{2}} \qquad (27)$$

All of the uncertainties are found from Table VII.

By definition, the Nusselt number is:

$$Nu = \frac{hD}{K_f}$$

and the second power equation for uncertainties of this equation is:

$$\frac{U_{Nu}}{Nu} = \left[\left[\frac{U_h}{h}\right]^2 + \left[\frac{U_D}{D}\right]^2 + \left[\frac{U_{K_f}}{K_f}\right]^2 \right]^{\frac{1}{2}} \qquad (28)$$

The values of $\left[\frac{U_D}{D}\right]^2$ and $\left[\frac{U_{K_f}}{K_f}\right]^2$ can be neglected.

Thus, equation (21) becomes:

$$\frac{U_{Nu}}{Nu} = \frac{U_h}{h} \qquad (29)$$

Using equation (15), section III, E2, to determine the uncertainty in the calculation of the Grashof number:

$$Gr = (g\beta/\nu 2)\, D^3\, (T_s - T_b)$$

and

$$\frac{U_{Gr}}{Gr} = \left[\left[\frac{U_{g\beta/\nu 2}}{g\beta/\nu 2}\right]^2 + \left[\frac{3\ U_D}{D}\right]^2 + \left[\frac{U_{\delta T}}{\delta T}\right]^2 \right]^{\frac{1}{2}} \qquad (30)$$

For Freon 113, using equation (17), section II, A3, to determine the uncertainty in calculation of the Grashof number:

$$Gr = (173135.52)(\beta)(\rho/\nu)^2\ \delta T$$

and

$$\frac{U_{Gr}}{Gr} = \left[\left[\frac{U_\beta}{\beta}\right]^2 + \left[\frac{2U_\rho}{\rho}\right]^2 + \left[\frac{2U_\mu}{\mu}\right]^2 + \left[\frac{U_{\delta T}}{\delta T}\right]^2 \right]^{\frac{1}{2}} \qquad (31)$$

All of the uncertainties are found from Table VII.

Using equation (16), section III, E2, to determine the uncertainty in the calculation of the Rayleigh number:

$$Ra = Gr \cdot Pr$$

and

$$\frac{U_{Ra}}{Ra} = \left[\left[\frac{U_{Gr}}{Gr}\right]^2 + \left[\frac{U_{Pr}}{Pr}\right]^2 \right]^{\frac{1}{2}} \qquad \text{(for } H_2O\text{)} \qquad (32)$$

For Freon 113, by definition

$$Pr = \frac{\mu Cp}{K_f}$$

and uncertainty in the calculation of the Prandlt is:

$$\frac{U_{Pr}}{Pr} = \left[\left[\frac{U_\mu}{\mu}\right]^2 + \left[\frac{U_{Cp}}{Cp}\right]^2 + \left[\frac{U_{K_f}}{K_f}\right]^2 \right]^{\frac{1}{2}}$$

All of the uncertainties are found from Table VII.

Thus, for Freon 113, we have

$$\frac{U_{Ra}}{Ra} = \left[\left[\frac{U_{Gr}}{Gr}\right]^2 + \left[\frac{U_\mu}{\mu}\right]^2 + \left[\frac{U_{Cp}}{Cp}\right]^2 + \left[\frac{U_{K_f}}{K_f}\right]^2 \right]^{\frac{1}{2}}$$

A summary of the results of this analysis is in Table I for water with seven-hole test section and Table II for Freon 113 with seven-hole test section.

BIBLIOGRAPHY

1. Marto, J. A., Moulson, J. A., Maynard, M. D., "Nucleate Pool Boiling of Nitrogen With Different Surface Conditions," J. of Heat Transfer, v. 90, p. 437-444, November 1968.
2. Ostrach, S., "New Aspects of Natural Convection Heat-Transfer," Trans. ASME, v. 75, p. 1287-1290, 1953.
3. O'Connor, J. M., Natural Convection Flow Visualization and Heat Transfer From a Horizontal Circular Disk, M.S. Thesis, Naval Postgraduate School, Monterey, California, June 1974.
4. Lord Rayleigh, "On Convection Currents in a Horizontal Layer of Fluid When the Higher Temperature is on The Under Sides," Phil. Mag, v. 32, p. 529, 1916.
5. Jeffreys, H., "Some Cases of Instability in Fluid Motion," Proc. Roy. Soc. (London), v. 118(A), p. 195, 1928.
6. Low, A. R., "On the Criterion for Stability of a Layer of Viscous Fluid Heated From Below," Proc. Roy. Soc. (London), v. 125(A), p. 180, 1929.
7. Schmidt, R. J., and Saunders, O. A., "On the Motion of a Fluid Heated From Below," Proc. Roy. Soc. (London), v. 165(A), p. 216, 1935.
8. Soberman, R. K., "Effects of Lateral Boundaries on Natural Convection," J. App. Phy., v. 29, p. 872, 1958.
9. ERK, D.S., Fundamentals of Heat Transfer, 1961, 2ed., McGraw Hill, Series in Mechanical Engineering, 1961.
10. Mull, W., and Reiber, H., "Der Warmeschutz von Luftschichten," Beihefte Gesundh.-Ing., Ser. 1, no. 28, 1930.
11. Torrance, K. E., Orloff, L., and Rockett, J. A., "Experiments on Natural Convection in Enclosures with Localized Heating From Below," Journal of Fluid Mechanics, v. 36, part 1, p. 21-23, 1969
12. Torrance, K. E., Orloff, L., and Rockett, J. A., "Numerical Study of Natural Convection in a Enclosure With Localized Heating From Below-Creeping Flow to the Onset of Laminar Instability," J. of Fluid Mechanics, v. 36, part 1, p. 33-54, 1969.

13. Lee, S. L., and Hellman, J. M., Advances in Heat Transfer, v. 10, p. 220-281, 1974.

14. Duncan, D. S., Natural Convection Heat Transfer From a Horizontal Disk in a Cylindrical Enclosure, M. S. Thesis, Naval Postgraduate School, Monterey, California, 1971.

15. Moulson, J. A., Nucleate Pool Boiling of Nitrogen From Artificials Cavities, M. S. Thesis, Naval Postgraduate School, Monterey, California, 1967.

16. Mac Kenzie, D. K., Vaporization of Thin Liquid Films, M. S. Thesis, Naval Postgraduate School, Monterey, California, 1972.

17. Touloukian and De Hitt, Thermophysical Properties of Matter, v. 1, 1970.

18. Kreith, F., Principles of Heat Transfer, Table A-3, Appendix III, 3rd edition, p. 638.

19. Thermophysical Properties of Refrigerants, 2nd edition, ASHRAE, 1973.

20. Streeter, V. L., Fluid Mechanics, 5th edition, Mac Graw-Hill, 1971.

21. Kline, S. J., and Mac Clintock, F. A., "Describing Uncertainties in Simple Experiments," Mechanical Engineering, V. 75, p. 3-8, January 1953.

INITIAL DISTRIBUTION LIST

		No. Copies
1.	Defense Documentation Center Cameron Station Alexandria, Virginia 22314	2
2.	Library, Code 0202 Naval Postgraduate School Monterey, California 93940	2
3.	Assoc. Professor M. D. Kelleher Department of Mechanical Engineering Naval Postgraduate School Monterey, California 93940	2
4.	Le Vinh Hiep 487 Watson Street #1 Monterey, California 93940	2
5.	Department Chairman, Code 59 Department of Mechanical Engineering Naval Postgraduate School Monterey, California 93940	2

16134)

Thesis
H52735 Hiep
c.1

The influence of drilled cavities on natural convection heat transfer from a horizontal surface.